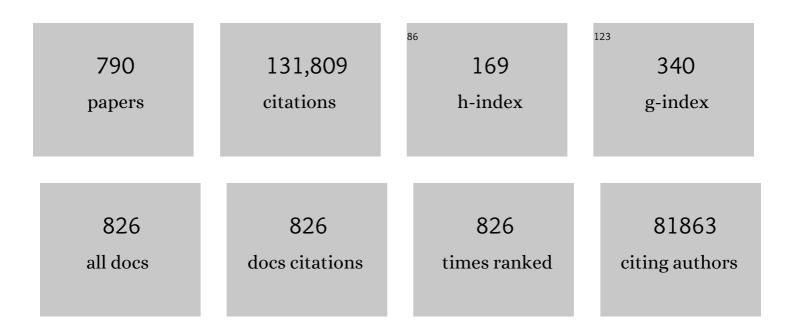
List of Publications by Year in descending order

Source: https://exaly.com/author-pdf/4975007/publications.pdf Version: 2024-02-01



#	Article	IF	CITATIONS
1	The reduction of graphene oxide. Carbon, 2012, 50, 3210-3228.	5.4	4,247
2	Advanced Materials for Energy Storage. Advanced Materials, 2010, 22, E28-62.	11.1	4,168
3	Three-dimensional flexible and conductive interconnected graphene networks grown by chemical vapour deposition. Nature Materials, 2011, 10, 424-428.	13.3	3,493
4	Grapheneâ€Like Carbon Nitride Nanosheets for Improved Photocatalytic Activities. Advanced Functional Materials, 2012, 22, 4763-4770.	7.8	3,009
5	Graphene Anchored with Co ₃ O ₄ Nanoparticles as Anode of Lithium Ion Batteries with Enhanced Reversible Capacity and Cyclic Performance. ACS Nano, 2010, 4, 3187-3194.	7.3	2,358
6	Doped Graphene Sheets As Anode Materials with Superhigh Rate and Large Capacity for Lithium Ion Batteries. ACS Nano, 2011, 5, 5463-5471.	7.3	1,904
7	Unique Electronic Structure Induced High Photoreactivity of Sulfur-Doped Graphitic C ₃ N ₄ . Journal of the American Chemical Society, 2010, 132, 11642-11648.	6.6	1,856
8	Hydrogen Storage in Single-Walled Carbon Nanotubes at Room Temperature. Science, 1999, 286, 1127-1129.	6.0	1,795
9	Graphene-Wrapped Fe ₃ O ₄ Anode Material with Improved Reversible Capacity and Cyclic Stability for Lithium Ion Batteries. Chemistry of Materials, 2010, 22, 5306-5313.	3.2	1,773
10	3D Aperiodic Hierarchical Porous Graphitic Carbon Material for Highâ€Rate Electrochemical Capacitive Energy Storage. Angewandte Chemie - International Edition, 2008, 47, 373-376.	7.2	1,747
11	Lightweight and Flexible Graphene Foam Composites for Highâ€Performance Electromagnetic Interference Shielding. Advanced Materials, 2013, 25, 1296-1300.	11.1	1,703
12	Graphene/metal oxide composite electrode materials for energy storage. Nano Energy, 2012, 1, 107-131.	8.2	1,669
13	Fabrication of Graphene/Polyaniline Composite Paper <i>via In Situ</i> Anodic Electropolymerization for High-Performance Flexible Electrode. ACS Nano, 2009, 3, 1745-1752.	7.3	1,464
14	Direct reduction of graphene oxide films into highly conductive and flexible graphene films by hydrohalic acids. Carbon, 2010, 48, 4466-4474.	5.4	1,459
15	High-Energy MnO ₂ Nanowire/Graphene and Graphene Asymmetric Electrochemical Capacitors. ACS Nano, 2010, 4, 5835-5842.	7.3	1,448
16	More Reliable Lithiumâ€6ulfur Batteries: Status, Solutions and Prospects. Advanced Materials, 2017, 29, 1606823.	11.1	1,414
17	Progress in flexible lithium batteries and future prospects. Energy and Environmental Science, 2014, 7, 1307-1338.	15.6	1,312
18	Fluorographene: A Twoâ€Dimensional Counterpart of Teflon. Small, 2010, 6, 2877-2884.	5.2	1,146

#	Article	IF	CITATIONS
19	Anchoring Hydrous RuO ₂ on Graphene Sheets for Highâ€Performance Electrochemical Capacitors. Advanced Functional Materials, 2010, 20, 3595-3602.	7.8	1,122
20	On the True Photoreactivity Order of {001}, {010}, and {101} Facets of Anatase TiO ₂ Crystals. Angewandte Chemie - International Edition, 2011, 50, 2133-2137.	7.2	1,106
21	Large-area high-quality 2D ultrathin Mo2C superconducting crystals. Nature Materials, 2015, 14, 1135-1141.	13.3	1,045
22	Titania-based photocatalysts—crystal growth, doping and heterostructuring. Journal of Materials Chemistry, 2010, 20, 831-843.	6.7	1,028
23	Chemical Vapor Deposition Growth and Applications of Two-Dimensional Materials and Their Heterostructures. Chemical Reviews, 2018, 118, 6091-6133.	23.0	1,000
24	Repeated growth and bubbling transfer of graphene with millimetre-size single-crystal grains using platinum. Nature Communications, 2012, 3, 699.	5.8	985
25	Oxygen Bridges between NiO Nanosheets and Graphene for Improvement of Lithium Storage. ACS Nano, 2012, 6, 3214-3223.	7.3	977
26	Reversible calcium alloying enables a practical room-temperature rechargeable calcium-ion battery with a high discharge voltage. Nature Chemistry, 2018, 10, 667-672.	6.6	971
27	Titanium Dioxide Crystals with Tailored Facets. Chemical Reviews, 2014, 114, 9559-9612.	23.0	922
28	Conductive porous vanadium nitride/graphene composite as chemical anchor of polysulfides for lithium-sulfur batteries. Nature Communications, 2017, 8, 14627.	5.8	912
29	A Graphene–Pure‣ulfur Sandwich Structure for Ultrafast, Long‣ife Lithium–Sulfur Batteries. Advanced Materials, 2014, 26, 625-631.	11.1	908
30	Efficient Preparation of Large-Area Graphene Oxide Sheets for Transparent Conductive Films. ACS Nano, 2010, 4, 5245-5252.	7.3	869
31	Selfâ€Assembled Freeâ€&tanding Graphite Oxide Membrane. Advanced Materials, 2009, 21, 3007-3011.	11.1	868
32	Crystal facet engineering of semiconductor photocatalysts: motivations, advances and unique properties. Chemical Communications, 2011, 47, 6763.	2.2	867
33	Graphene–Cellulose Paper Flexible Supercapacitors. Advanced Energy Materials, 2011, 1, 917-922.	10.2	831
34	Synthesis of Graphene Sheets with High Electrical Conductivity and Good Thermal Stability by Hydrogen Arc Discharge Exfoliation. ACS Nano, 2009, 3, 411-417.	7.3	807
35	An Amorphous Carbon Nitride Photocatalyst with Greatly Extended Visibleâ€Lightâ€Responsive Range for Photocatalytic Hydrogen Generation. Advanced Materials, 2015, 27, 4572-4577.	11.1	771
36	Carbon–sulfur composites for Li–S batteries: status and prospects. Journal of Materials Chemistry A, 2013, 1, 9382.	5.2	757

#	Article	IF	CITATIONS
37	Flexible graphene-based lithium ion batteries with ultrafast charge and discharge rates. Proceedings of the United States of America, 2012, 109, 17360-17365.	3.3	728
38	Fibrous Hybrid of Graphene and Sulfur Nanocrystals for High-Performance Lithium–Sulfur Batteries. ACS Nano, 2013, 7, 5367-5375.	7.3	722
39	Large-scale and low-cost synthesis of single-walled carbon nanotubes by the catalytic pyrolysis of hydrocarbons. Applied Physics Letters, 1998, 72, 3282-3284.	1.5	678
40	Purification of carbon nanotubes. Carbon, 2008, 46, 2003-2025.	5.4	660
41	Increasing the Visible Light Absorption of Graphitic Carbon Nitride (Melon) Photocatalysts by Homogeneous Selfâ€Modification with Nitrogen Vacancies. Advanced Materials, 2014, 26, 8046-8052.	11.1	658
42	Synthesis of high-quality graphene with a pre-determined number of layers. Carbon, 2009, 47, 493-499.	5.4	650
43	Field Emission of Singleâ€Layer Graphene Films Prepared by Electrophoretic Deposition. Advanced Materials, 2009, 21, 1756-1760.	11.1	624
44	Battery Performance and Photocatalytic Activity of Mesoporous Anatase TiO ₂ Nanospheres/Graphene Composites by Templateâ€Free Selfâ€Assembly. Advanced Functional Materials, 2011, 21, 1717-1722.	7.8	601
45	Carbon Nanotubes and Graphene for Flexible Electrochemical Energy Storage: from Materials to Devices. Advanced Materials, 2016, 28, 4306-4337.	11.1	595
46	Visible Light Responsive Nitrogen Doped Anatase TiO ₂ Sheets with Dominant {001} Facets Derived from TiN. Journal of the American Chemical Society, 2009, 131, 12868-12869.	6.6	570
47	Nitrogen Vacancy-Promoted Photocatalytic Activity of Graphitic Carbon Nitride. Journal of Physical Chemistry C, 2012, 116, 11013-11018.	1.5	570
48	Chemical vapor deposition of layered two-dimensional MoSi ₂ N ₄ materials. Science, 2020, 369, 670-674.	6.0	556
49	A Flexible Sulfurâ€Grapheneâ€Polypropylene Separator Integrated Electrode for Advanced Li–S Batteries. Advanced Materials, 2015, 27, 641-647.	11.1	545
50	The Fabrication, Properties, and Uses of Graphene/Polymer Composites. Macromolecular Chemistry and Physics, 2012, 213, 1060-1077.	1.1	537
51	Hydrogen storage in carbon nanotubes. Carbon, 2001, 39, 1447-1454.	5.4	532
52	A graphene foam electrode with high sulfur loading for flexible and high energy Li-S batteries. Nano Energy, 2015, 11, 356-365.	8.2	526
53	Synthesis and Electrochemical Property of Boron-Doped Mesoporous Carbon in Supercapacitor. Chemistry of Materials, 2008, 20, 7195-7200.	3.2	511
54	Selective Breaking of Hydrogen Bonds of Layered Carbon Nitride for Visible Light Photocatalysis. Advanced Materials, 2016, 28, 6471-6477.	11.1	507

HUI-MING CHENG

#	Article	IF	CITATIONS
55	Hollow Nanostructures for Photocatalysis: Advantages and Challenges. Advanced Materials, 2019, 31, e1801369.	11.1	506
56	Carbon materials for Li–S batteries: Functional evolution and performance improvement. Energy Storage Materials, 2016, 2, 76-106.	9.5	504
57	High Sensitivity Gas Detection Using a Macroscopic Three-Dimensional Graphene Foam Network. Scientific Reports, 2011, 1, 166.	1.6	503
58	3D Grapheneâ€Foam–Reducedâ€Grapheneâ€Oxide Hybrid Nested Hierarchical Networks for Highâ€Performanc Li–S Batteries. Advanced Materials, 2016, 28, 1603-1609.	e 11.1	497
59	3D Interconnected Electrode Materials with Ultrahigh Areal Sulfur Loading for Li–S Batteries. Advanced Materials, 2016, 28, 3374-3382.	11.1	488
60	Synergistic Effects of B/N Doping on the Visible‣ight Photocatalytic Activity of Mesoporous TiO ₂ . Angewandte Chemie - International Edition, 2008, 47, 4516-4520.	7.2	484
61	Graphene sponge for efficient and repeatable adsorption and desorption of water contaminations. Journal of Materials Chemistry, 2012, 22, 20197.	6.7	478
62	Enhanced photocatalytic hydrogen evolution by prolonging the lifetime of carriers in ZnO/CdS heterostructures. Chemical Communications, 2009, , 3452.	2.2	476
63	Incorporation of Graphenes in Nanostructured TiO ₂ Films <i>via</i> Molecular Grafting for Dye-Sensitized Solar Cell Application. ACS Nano, 2010, 4, 3482-3488.	7.3	471
64	A flexible nanostructured sulphur–carbon nanotube cathode with high rate performance for Li-S batteries. Energy and Environmental Science, 2012, 5, 8901.	15.6	468
65	Green synthesis of graphene oxide byÂseconds timescale water electrolytic oxidation. Nature Communications, 2018, 9, 145.	5.8	468
66	Atomically Dispersed Transition Metals on Carbon Nanotubes with Ultrahigh Loading for Selective Electrochemical Carbon Dioxide Reduction. Advanced Materials, 2018, 30, e1706287.	11.1	459
67	Preparation of 2D material dispersions and their applications. Chemical Society Reviews, 2018, 47, 6224-6266.	18.7	459
68	Hierarchical porous nickel oxide and carbon as electrode materials for asymmetric supercapacitor. Journal of Power Sources, 2008, 185, 1563-1568.	4.0	439
69	Morphology and surface chemistry engineering toward pH-universal catalysts for hydrogen evolution at high current density. Nature Communications, 2019, 10, 269.	5.8	431
70	Highly stable graphene-oxide-based membranes with superior permeability. Nature Communications, 2018, 9, 1486.	5.8	428
71	Biological technologies for the remediation of co-contaminated soil. Critical Reviews in Biotechnology, 2017, 37, 1062-1076.	5.1	423
72	α-Sulfur Crystals as a Visible-Light-Active Photocatalyst. Journal of the American Chemical Society, 2012, 134, 9070-9073.	6.6	422

#	Article	IF	CITATIONS
73	Ligand-assisted cation-exchange engineering for high-efficiency colloidal Cs1â^'xFAxPbI3 quantum dot solar cells with reduced phase segregation. Nature Energy, 2020, 5, 79-88.	19.8	412
74	Nanosized anatase TiO2 single crystals for enhanced photocatalytic activity. Chemical Communications, 2010, 46, 755-757.	2.2	403
75	Facile Hydrothermal Synthesis of <i>Z</i> -Scheme Bi ₂ Fe ₄ O ₉ /Bi ₂ WO ₆ Heterojunction Photocatalyst with Enhanced Visible Light Photocatalytic Activity. ACS Applied Materials & amp; Interfaces. 2018. 10. 18824-18836.	4.0	397
76	The global growth of graphene. Nature Nanotechnology, 2014, 9, 726-730.	15.6	391
77	Carbon Nanotubes and Related Nanomaterials: Critical Advances and Challenges for Synthesis toward Mainstream Commercial Applications. ACS Nano, 2018, 12, 11756-11784.	7.3	388
78	A red anatase TiO2 photocatalyst for solar energy conversion. Energy and Environmental Science, 2012, 5, 9603.	15.6	379
79	CdS–mesoporous ZnS core–shell particles for efficient and stable photocatalytic hydrogen evolution under visible light. Energy and Environmental Science, 2014, 7, 1895.	15.6	379
80	Enhanced Photoactivity of Oxygen-Deficient Anatase TiO ₂ Sheets with Dominant {001} Facets. Journal of Physical Chemistry C, 2009, 113, 21784-21788.	1.5	376
81	Air-stable and freestanding lithium alloy/graphene foil as an alternative to lithium metal anodes. Nature Nanotechnology, 2017, 12, 993-999.	15.6	376
82	Nitrogenâ€Doped Carbon Monolith for Alkaline Supercapacitors and Understanding Nitrogenâ€Induced Redox Transitions. Chemistry - A European Journal, 2012, 18, 5345-5351.	1.7	358
83	Crystal facet-dependent photocatalytic oxidation and reduction reactivity of monoclinic WO3 for solar energy conversion. Journal of Materials Chemistry, 2012, 22, 6746.	6.7	356
84	Two-Dimensional Materials for Thermal Management Applications. Joule, 2018, 2, 442-463.	11.7	353
85	Overview of the synthesis of MXenes and other ultrathin 2D transition metal carbides and nitrides. Current Opinion in Solid State and Materials Science, 2019, 23, 149-163.	5.6	353
86	25th Anniversary Article: Carbon Nanotube―and Grapheneâ€Based Transparent Conductive Films for Optoelectronic Devices. Advanced Materials, 2014, 26, 1958-1991.	11.1	350
87	Ultra-thick graphene bulk supercapacitor electrodes for compact energy storage. Energy and Environmental Science, 2016, 9, 3135-3142.	15.6	347
88	Understanding the interactions between lithium polysulfides and N-doped graphene using density functional theory calculations. Nano Energy, 2016, 25, 203-210.	8.2	347
89	The Regulating Role of Carbon Nanotubes and Graphene in Lithiumâ€lon and Lithium–Sulfur Batteries. Advanced Materials, 2019, 31, e1800863.	11.1	339
90	Large-area synthesis of high-quality and uniform monolayer WS2 on reusable Au foils. Nature Communications, 2015, 6, 8569.	5.8	336

#	Article	IF	CITATIONS
91	Scalable Clean Exfoliation of Highâ€Quality Few‣ayer Black Phosphorus for a Flexible Lithium Ion Battery. Advanced Materials, 2016, 28, 510-517.	11.1	336
92	Carbon-Based Fibers for Advanced Electrochemical Energy Storage Devices. Chemical Reviews, 2020, 120, 2811-2878.	23.0	334
93	Flexible layer-structured Bi2Te3 thermoelectric on a carbon nanotube scaffold. Nature Materials, 2019, 18, 62-68.	13.3	316
94	One-Step Device Fabrication of Phosphorene and Graphene Interdigital Micro-Supercapacitors with High Energy Density. ACS Nano, 2017, 11, 7284-7292.	7.3	312
95	Megamerger in photocatalytic field: 2D g-C3N4 nanosheets serve as support of 0D nanomaterials for improving photocatalytic performance. Applied Catalysis B: Environmental, 2019, 240, 153-173.	10.8	310
96	Superhigh Electromagnetic Interference Shielding of Ultrathin Aligned Pristine Graphene Nanosheets Film. Advanced Materials, 2020, 32, e1907411.	11.1	310
97	Vertically Aligned Carbon Nanotubes Grown on Graphene Paper as Electrodes in Lithiumâ€lon Batteries and Dye‣ensitized Solar Cells. Advanced Energy Materials, 2011, 1, 486-490.	10.2	309
98	Tensile strength of single-walled carbon nanotubes directly measured from their macroscopic ropes. Applied Physics Letters, 2000, 77, 3161-3163.	1.5	306
99	Nanosized Li4Ti5O12/graphene hybrid materials with low polarization for high rate lithium ion batteries. Journal of Power Sources, 2011, 196, 8610-8617.	4.0	306
100	Two-Dimensional MoS ₂ Confined Co(OH) ₂ Electrocatalysts for Hydrogen Evolution in Alkaline Electrolytes. ACS Nano, 2018, 12, 4565-4573.	7.3	302
101	Vertically Aligned p-Type Single-Crystalline GaN Nanorod Arrays on n-Type Si for Heterojunction Photovoltaic Cells. Nano Letters, 2008, 8, 4191-4195.	4.5	298
102	Recent advances in graphene-based planar micro-supercapacitors for on-chip energy storage. National Science Review, 2014, 1, 277-292.	4.6	298
103	Self-assembled CdS/Au/ZnO heterostructure induced by surface polar charges for efficient photocatalytic hydrogen evolution. Journal of Materials Chemistry A, 2013, 1, 2773.	5.2	294
104	Phosphorene as a Polysulfide Immobilizer and Catalyst in Highâ€Performance Lithium–Sulfur Batteries. Advanced Materials, 2017, 29, 1602734.	11.1	289
105	Fabrication of novel magnetic MnFe2O4/bio-char composite and heterogeneous photo-Fenton degradation of tetracycline in near neutral pH. Chemosphere, 2019, 224, 910-921.	4.2	287
106	Band-to-Band Visible-Light Photon Excitation and Photoactivity Induced by Homogeneous Nitrogen Doping in Layered Titanates. Chemistry of Materials, 2009, 21, 1266-1274.	3.2	284
107	The Rechargeable Aluminum Battery: Opportunities and Challenges. Angewandte Chemie - International Edition, 2019, 58, 11978-11996.	7.2	276
108	A microporous–mesoporous carbon with graphitic structure for a high-rate stable sulfur cathode in carbonate solvent-based Li–S batteries. Physical Chemistry Chemical Physics, 2012, 14, 8703.	1.3	273

HUI-MING CHENG

#	Article	IF	CITATIONS
109	A Review of Carbon Nanotube―and Grapheneâ€Based Flexible Thinâ€Film Transistors. Small, 2013, 9, 1188-1205.	5.2	268
110	Graphitic Carbon Nitride-Based Heterojunction Photoactive Nanocomposites: Applications and Mechanism Insight. ACS Applied Materials & Interfaces, 2018, 10, 21035-21055.	4.0	266
111	Artificial Z-scheme photocatalytic system: What have been done and where to go?. Coordination Chemistry Reviews, 2019, 385, 44-80.	9.5	265
112	A 3D bi-functional porous N-doped carbon microtube sponge electrocatalyst for oxygen reduction and oxygen evolution reactions. Energy and Environmental Science, 2016, 9, 3079-3084.	15.6	260
113	Graphene-based materials for high-voltage and high-energy asymmetric supercapacitors. Energy Storage Materials, 2017, 6, 70-97.	9.5	260
114	Metal-Catalyst-Free Growth of Single-Walled Carbon Nanotubes. Journal of the American Chemical Society, 2009, 131, 2082-2083.	6.6	258
115	Key Aspects of Lithium Metal Anodes for Lithium Metal Batteries. Small, 2019, 15, e1900687.	5.2	253
116	Semiconductor-based photocatalysts for photocatalytic and photoelectrochemical water splitting: will we stop with photocorrosion?. Journal of Materials Chemistry A, 2020, 8, 2286-2322.	5.2	251
117	In Situ Grown Agl/Bi ₁₂ O ₁₇ Cl ₂ Heterojunction Photocatalysts for Visible Light Degradation of Sulfamethazine: Efficiency, Pathway, and Mechanism. ACS Sustainable Chemistry and Engineering, 2018, 6, 4174-4184.	3.2	249
118	Stabilized Nanoscale Zerovalent Iron Mediated Cadmium Accumulation and Oxidative Damage of <i>Boehmeria nivea</i> (L.) Gaudich Cultivated in Cadmium Contaminated Sediments. Environmental Science & Technology, 2017, 51, 11308-11316.	4.6	248
119	Toward More Reliable Lithium–Sulfur Batteries: An All-Graphene Cathode Structure. ACS Nano, 2016, 10, 8676-8682.	7.3	246
120	Metal–Organic Frameworks (MOFs)â€Derived Nitrogenâ€Doped Porous Carbon Anchored on Graphene with Multifunctional Effects for Lithium–Sulfur Batteries. Advanced Functional Materials, 2018, 28, 1707592.	7.8	246
121	Homogeneous and Fast Ion Conduction of PEOâ€Based Solidâ€State Electrolyte at Low Temperature. Advanced Functional Materials, 2020, 30, 2007172.	7.8	246
122	Tunable Band Gaps and p-Type Transport Properties of Boron-Doped Graphenes by Controllable Ion Doping Using Reactive Microwave Plasma. ACS Nano, 2012, 6, 1970-1978.	7.3	244
123	Strategies towards Low ost Dualâ€Ion Batteries with High Performance. Angewandte Chemie - International Edition, 2020, 59, 3802-3832.	7.2	242
124	Elemental superdoping of graphene and carbon nanotubes. Nature Communications, 2016, 7, 10921.	5.8	238
125	Visible Light Photocatalyst:Â Iodine-Doped Mesoporous Titania with a Bicrystalline Framework. Journal of Physical Chemistry B, 2006, 110, 20823-20828.	1.2	236
126	Metal/Oxide Interface Nanostructures Generated by Surface Segregation for Electrocatalysis. Nano Letters, 2015, 15, 7704-7710.	4.5	233

#	Article	IF	CITATIONS
127	An Unusual Strong Visibleâ€Light Absorption Band in Red Anatase TiO ₂ Photocatalyst Induced by Atomic Hydrogenâ€Occupied Oxygen Vacancies. Advanced Materials, 2018, 30, 1704479.	11.1	231
128	Nitrogenâ€6uperdoped 3D Graphene Networks for Highâ€Performance Supercapacitors. Advanced Materials, 2017, 29, 1701677.	11.1	230
129	Stable photocatalytic hydrogen evolution from water over ZnO–CdS core–shell nanorods. International Journal of Hydrogen Energy, 2010, 35, 8199-8205.	3.8	229
130	Mass production and industrial applications of graphene materials. National Science Review, 2018, 5, 90-101.	4.6	222
131	Polarized Raman Study of Single-Wall Semiconducting Carbon Nanotubes. Physical Review Letters, 2000, 85, 2617-2620.	2.9	221
132	Simultaneous Production and Functionalization of Boron Nitride Nanosheets by Sugarâ€Assisted Mechanochemical Exfoliation. Advanced Materials, 2019, 31, e1804810.	11.1	220
133	Adsorption and capillarity of nitrogen in aggregated multi-walled carbon nanotubes. Chemical Physics Letters, 2001, 345, 18-24.	1.2	213
134	Edge-controlled growth and kinetics of single-crystal graphene domains by chemical vapor deposition. Proceedings of the National Academy of Sciences of the United States of America, 2013, 110, 20386-20391.	3.3	213
135	Engineering <i>dâ€p</i> Orbital Hybridization in Singleâ€Atom Metalâ€Embedded Threeâ€Dimensional Electrodes for Li–S Batteries. Advanced Materials, 2021, 33, e2105947.	11.1	209
136	Repeated and Controlled Growth of Monolayer, Bilayer and Few-Layer Hexagonal Boron Nitride on Pt Foils. ACS Nano, 2013, 7, 5199-5206.	7.3	206
137	Hydrogen adsorption behavior of graphene above critical temperature. International Journal of Hydrogen Energy, 2009, 34, 2329-2332.	3.8	203
138	A Sulfurâ€Rich Copolymer@CNT Hybrid Cathode with Dualâ€Confinement of Polysulfides for Highâ€Performance Lithium–Sulfur Batteries. Advanced Materials, 2017, 29, 1603835.	11.1	202
139	Intercalated architecture of MA2Z4 family layered van der Waals materials with emerging topological, magnetic and superconducting properties. Nature Communications, 2021, 12, 2361.	5.8	199
140	Graphene: a promising 2D material for electrochemical energy storage. Science Bulletin, 2017, 62, 724-740.	4.3	198
141	A flexible ultrasensitive optoelectronic sensor array for neuromorphic vision systems. Nature Communications, 2021, 12, 1798.	5.8	198
142	Synthesis of anatase TiO2 rods with dominant reactive {010} facets for the photoreduction of CO2 to CH4 and use in dye-sensitized solar cells. Chemical Communications, 2011, 47, 8361.	2.2	196
143	Comparison of the rate capability of nanostructured amorphous and anatase TiO ₂ for lithium insertion using anodic TiO ₂ nanotube arrays. Nanotechnology, 2009, 20, 225701.	1.3	194
144	Novel Boron Nitride Hollow Nanoribbons. ACS Nano, 2008, 2, 2183-2191.	7.3	192

#	Article	IF	CITATIONS
145	Switching the selectivity of the photoreduction reaction of carbon dioxide by controlling the band structure of a g-C ₃ N ₄ photocatalyst. Chemical Communications, 2014, 50, 10837.	2.2	192
146	Ultrahigh-voltage integrated micro-supercapacitors with designable shapes and superior flexibility. Energy and Environmental Science, 2019, 12, 1534-1541.	15.6	192
147	ZnO–CdS@Cd Heterostructure for Effective Photocatalytic Hydrogen Generation. Advanced Energy Materials, 2012, 2, 42-46.	10.2	191
148	Hydrogen storage in carbon nanotubes revisited. Carbon, 2010, 48, 452-455.	5.4	190
149	Carbonâ€Based Metalâ€Free Catalysts for Energy Storage and Environmental Remediation. Advanced Materials, 2019, 31, e1806128.	11.1	188
150	An Anionâ€Tuned Solid Electrolyte Interphase with Fast Ion Transfer Kinetics for Stable Lithium Anodes. Advanced Energy Materials, 2020, 10, 1903843.	10.2	186
151	Rosin-enabled ultraclean and damage-free transfer of graphene for large-area flexible organic light-emitting diodes. Nature Communications, 2017, 8, 14560.	5.8	184
152	Ammonia Borane Destabilized by Lithium Hydride: An Advanced Onâ€Board Hydrogen Storage Material. Advanced Materials, 2008, 20, 2756-2759.	11.1	183
153	Superhydrophobic Graphene Foams. Small, 2013, 9, 75-80.	5.2	183
154	Enhanced Photocatalytic H ₂ Production in Core–Shell Engineered Rutile TiO ₂ . Advanced Materials, 2016, 28, 5850-5856.	11.1	183
155	Single-wall carbon nanotube network enabled ultrahigh sulfur-content electrodes for high-performance lithium-sulfur batteries. Nano Energy, 2017, 42, 205-214.	8.2	183
156	CuS Microspheres with Tunable Interlayer Space and Micropore as a Highâ€Rate and Longâ€Life Anode for Sodiumâ€Ion Batteries. Advanced Energy Materials, 2018, 8, 1800930.	10.2	183
157	Amorphous cobalt–boron/nickel foam as an effective catalyst for hydrogen generation from alkaline sodium borohydride solution. Journal of Power Sources, 2008, 177, 17-23.	4.0	181
158	The Chemistry and Promising Applications of Graphene and Porous Graphene Materials. Advanced Functional Materials, 2020, 30, 1909035.	7.8	181
159	A highly reversible Co3S4 microsphere cathode material for aluminum-ion batteries. Nano Energy, 2019, 56, 100-108.	8.2	179
160	Amorphous TiO ₂ nanotube arrays for low-temperature oxygen sensors. Nanotechnology, 2008, 19, 405504.	1.3	178
161	Ultrahigh-performance transparent conductive films of carbon-welded isolated single-wall carbon nanotubes. Science Advances, 2018, 4, eaap9264.	4.7	178
162	Unique physicochemical properties of two-dimensional light absorbers facilitating photocatalysis. Chemical Society Reviews, 2018, 47, 6410-6444.	18.7	178

#	Article	IF	CITATIONS
163	Efficient growth of high-quality graphene films on Cu foils by ambient pressure chemical vapor deposition. Applied Physics Letters, 2010, 97, .	1.5	176
164	Scalable Fabrication of Photochemically Reduced Graphene-Based Monolithic Micro-Supercapacitors with Superior Energy and Power Densities. ACS Nano, 2017, 11, 4283-4291.	7.3	176
165	Hydrogen uptake in vapor-grown carbon nanofibers. Carbon, 1999, 37, 1649-1652.	5.4	173
166	Synthesis and upconversion luminescence of N-doped graphene quantum dots. Applied Physics Letters, 2012, 101, .	1.5	173
167	Synergistic Effect of Aligned Graphene Nanosheets in Graphene Foam for Highâ€Performance Thermally Conductive Composites. Advanced Materials, 2019, 31, e1900199.	11.1	173
168	Hollow Anatase TiO ₂ Single Crystals and Mesocrystals with Dominant {101} Facets for Improved Photocatalysis Activity and Tuned Reaction Preference. ACS Catalysis, 2012, 2, 1854-1859.	5.5	172
169	Scalable non-liquid-crystal spinning of locally aligned graphene fibers for high-performance wearable supercapacitors. Nano Energy, 2015, 15, 642-653.	8.2	172
170	Effects of calcium at toxic concentrations of cadmium in plants. Planta, 2017, 245, 863-873.	1.6	169
171	Critical review of recent progress of flexible perovskite solar cells. Materials Today, 2020, 39, 66-88.	8.3	169
172	Metal sulfide/MOF-based composites as visible-light-driven photocatalysts for enhanced hydrogen production from water splitting. Coordination Chemistry Reviews, 2020, 409, 213220.	9.5	169
173	Hydrogen generation from sodium borohydride solution using a ruthenium supported on graphite catalyst. International Journal of Hydrogen Energy, 2010, 35, 3023-3028.	3.8	167
174	Efficient and scalable synthesis of highly aligned and compact two-dimensional nanosheet films with record performances. Nature Communications, 2018, 9, 3484.	5.8	165
175	Polymorph Evolution Mechanisms and Regulation Strategies of Lithium Metal Anode under Multiphysical Fields. Chemical Reviews, 2021, 121, 5986-6056.	23.0	165
176	Electrochemical interfacial capacitance in multilayer graphene sheets: Dependence on number of stacking layers. Electrochemistry Communications, 2009, 11, 1729-1732.	2.3	160
177	Controlled Electrochemical Charge Injection to Maximize the Energy Density of Supercapacitors. Angewandte Chemie - International Edition, 2013, 52, 3722-3725.	7.2	160
178	All-solid-state flexible planar lithium ion micro-capacitors. Energy and Environmental Science, 2018, 11, 2001-2009.	15.6	160
179	Hydrogen adsorption/desorption behavior of multi-walled carbon nanotubes with different diameters. Carbon, 2003, 41, 2471-2476.	5.4	158
180	Remediation of contaminated soils by biotechnology with nanomaterials: bio-behavior, applications, and perspectives. Critical Reviews in Biotechnology, 2018, 38, 455-468.	5.1	158

#	Article	IF	CITATIONS
181	Polysulfide immobilization and conversion on a conductive polar MoC@MoOx material for lithium-sulfur batteries. Energy Storage Materials, 2018, 10, 56-61.	9.5	157
182	In-situ self-assembly construction of hollow tubular g-C3N4 isotype heterojunction for enhanced visible-light photocatalysis: Experiments and theories. Journal of Hazardous Materials, 2021, 401, 123355.	6.5	157
183	Lithiumâ€Catalyzed Dehydrogenation of Ammonia Borane within Mesoporous Carbon Framework for Chemical Hydrogen Storage. Advanced Functional Materials, 2009, 19, 265-271.	7.8	156
184	Swelling and mechanical behaviors of carbon nanotube/poly(vinyl alcohol) hybrid hydrogels. Materials Letters, 2007, 61, 1704-1706.	1.3	154
185	Tailoring the thermal and electrical transport properties of graphene films by grain size engineering. Nature Communications, 2017, 8, 14486.	5.8	154
186	An Aluminum–Sulfur Battery with a Fast Kinetic Response. Angewandte Chemie - International Edition, 2018, 57, 1898-1902.	7.2	154
187	A nanosized Fe2O3 decorated single-walled carbon nanotube membrane as a high-performance flexible anode for lithium ion batteries. Journal of Materials Chemistry, 2012, 22, 17942.	6.7	153
188	High-throughput production of cheap mineral-based two-dimensional electrocatalysts for high-current-density hydrogen evolution. Nature Communications, 2020, 11, 3724.	5.8	153
189	Free-standing integrated cathode derived from 3D graphene/carbon nanotube aerogels serving as binder-free sulfur host and interlayer for ultrahigh volumetric-energy-density lithium sulfur batteries. Nano Energy, 2019, 60, 743-751.	8.2	151
190	Purification of Single-Wall Carbon Nanotubes by Electrochemical Oxidation. Chemistry of Materials, 2004, 16, 5744-5750.	3.2	149
191	Kinetically Enhanced Electrochemical Redox of Polysulfides on Polymeric Carbon Nitrides for Improved Lithium–Sulfur Batteries. ACS Applied Materials & Interfaces, 2016, 8, 25193-25201.	4.0	149
192	Secondary-Atom-Assisted Synthesis of Single Iron Atoms Anchored on N-Doped Carbon Nanowires for Oxygen Reduction Reaction. ACS Catalysis, 2019, 9, 5929-5934.	5.5	149
193	Ultrathin 2D Transition Metal Carbides for Ultrafast Pulsed Fiber Lasers. ACS Photonics, 2018, 5, 1808-1816.	3.2	148
194	Polar interface-induced improvement in high photocatalytic hydrogen evolution over ZnO–CdS heterostructures. Energy and Environmental Science, 2011, 4, 3976.	15.6	147
195	Positive temperature coefficient effect in multiwalled carbon nanotube/high-density polyethylene composites. Applied Physics Letters, 2005, 86, 062112.	1.5	146
196	Effect of Pore Packing Defects in 2-D Ordered Mesoporous Carbons on Ionic Transport. Journal of Physical Chemistry B, 2006, 110, 8570-8575.	1.2	144
197	Constructing a Stable Interface Layer by Tailoring Solvation Chemistry in Carbonate Electrolytes for Highâ€Performance Lithiumâ€Metal Batteries. Advanced Materials, 2022, 34, e2108400.	11.1	144
198	Efficient synthesis of graphene nanoribbons sonochemically cut from graphene sheets. Nano Research, 2010, 3, 16-22.	5.8	143

#	Article	IF	CITATIONS
199	Controlled Vapor–Solid Deposition of Millimeterâ€Size Single Crystal 2D Bi ₂ O ₂ Se for Highâ€Performance Phototransistors. Advanced Functional Materials, 2019, 29, 1807979.	7.8	143
200	Structure-related electrochemical performance of organosulfur compounds for lithium–sulfur batteries. Energy and Environmental Science, 2020, 13, 1076-1095.	15.6	143
201	Purification of single-walled carbon nanotubes synthesized by the hydrogen arc-discharge method. Journal of Materials Research, 2001, 16, 2526-2529.	1.2	140
202	Morphology, diameter distribution and Raman scattering measurements of double-walled carbon nanotubes synthesized by catalytic decomposition of methane. Chemical Physics Letters, 2002, 359, 196-202.	1.2	139
203	Ultrafast Growth of Highâ€Quality Monolayer WSe ₂ on Au. Advanced Materials, 2017, 29, 1700990.	11.1	139
204	Monolithic Fe2O3/graphene hybrid for highly efficient lithium storage and arsenic removal. Carbon, 2014, 67, 500-507.	5.4	137
205	Total Color Difference for Rapid and Accurate Identification of Graphene. ACS Nano, 2008, 2, 1625-1633.	7.3	135
206	Bulk Synthesis of Large Diameter Semiconducting Single-Walled Carbon Nanotubes by Oxygen-Assisted Floating Catalyst Chemical Vapor Deposition. Journal of the American Chemical Society, 2011, 133, 5232-5235.	6.6	134
207	Stabilizing sulfur cathodes using nitrogen-doped graphene as a chemical immobilizer for Li S batteries. Carbon, 2016, 108, 120-126.	5.4	134
208	Metallic and Carbon Nanotube-Catalyzed Coupling of Hydrogenation in Magnesium. Journal of the American Chemical Society, 2007, 129, 15650-15654.	6.6	131
209	An aqueous dissolved polysulfide cathode for lithium–sulfur batteries. Energy and Environmental Science, 2014, 7, 3307-3312.	15.6	131
210	Controlling reduction degree of graphene oxide membranes for improved water permeance. Science Bulletin, 2018, 63, 788-794.	4.3	131
211	Reversible hydrogen storage in LiBH4 destabilized by milling with Al. Applied Physics A: Materials Science and Processing, 2007, 89, 963-966.	1.1	128
212	Heteroatomâ€Modulated Switching of Photocatalytic Hydrogen and Oxygen Evolution Preferences of Anatase TiO ₂ Microspheres. Advanced Functional Materials, 2012, 22, 3233-3238.	7.8	128
213	A Selfâ€6tanding and Flexible Electrode of Li ₄ Ti ₅ O ₁₂ Nanosheets with a Nâ€Doped Carbon Coating for High Rate Lithium Ion Batteries. Advanced Functional Materials, 2013, 23, 5429-5435.	7.8	128
214	Electron field emission of a nitrogen-doped TiO2nanotube array. Nanotechnology, 2008, 19, 025606.	1.3	127
215	lodine doped anatase TiO2 photocatalyst with ultra-long visible light response: correlation between geometric/electronic structures and mechanisms. Journal of Materials Chemistry, 2009, 19, 2822.	6.7	127
216	Insights into the deposition chemistry of Li ions in nonaqueous electrolyte for stable Li anodes. Chemical Society Reviews, 2021, 50, 3178-3210.	18.7	126

#	Article	IF	CITATIONS
217	A sandwich structure of graphene and nickel oxide with excellent supercapacitive performance. Journal of Materials Chemistry, 2011, 21, 9014.	6.7	125
218	Effects of oxygen vacancies on the electrochemical performance of tin oxide. Journal of Materials Chemistry A, 2013, 1, 1536-1539.	5.2	125
219	Selective Heterogeneous Nucleation and Growth of Size-Controlled Metal Nanoparticles on Carbon Nanotubes in Solution. Chemistry - A European Journal, 2006, 12, 2542-2549.	1.7	124
220	Arbitrary-Shaped Graphene-Based Planar Sandwich Supercapacitors on One Substrate with Enhanced Flexibility and Integration. ACS Nano, 2017, 11, 2171-2179.	7.3	121
221	Tantalum (oxy)nitride based photoanodes for solar-driven water oxidation. Journal of Materials Chemistry A, 2016, 4, 2783-2800.	5.2	120
222	CdPS ₃ nanosheets-based membrane with high proton conductivity enabled by Cd vacancies. Science, 2020, 370, 596-600.	6.0	120
223	Morphology, thermal stability, and dynamic mechanical properties of atactic polypropylene/carbon nanotube composites. Journal of Applied Polymer Science, 2005, 98, 1087-1091.	1.3	119
224	The growth of multi-walled carbon nanotubes with different morphologies on carbon fibers. Carbon, 2005, 43, 663-665.	5.4	118
225	Effects of carbon on hydrogen storage performances of hydrides. Journal of Materials Chemistry, 2010, 20, 5390.	6.7	116
226	Preparation and electrochemical property of Fe2O3 nanoparticles-filled carbon nanotubes. Chemical Communications, 2010, 46, 8576.	2.2	116
227	Importance of Oxygen in the Metal-Free Catalytic Growth of Single-Walled Carbon Nanotubes from SiO _{<i>x</i>} by a Vaporâ^'Solidâ^'Solid Mechanism. Journal of the American Chemical Society, 2011, 133, 197-199.	6.6	116
228	Efficient Promotion of Anatase TiO2 Photocatalysis via Bifunctional Surface-Terminating Tiâ^'Oâ^'Bâ^'N Structures. Journal of Physical Chemistry C, 2009, 113, 12317-12324.	1.5	115
229	Template-free synthesis of Ta3N5 nanorod arrays for efficient photoelectrochemical water splitting. Chemical Communications, 2013, 49, 3019.	2.2	115
230	Selective Chemical Epitaxial Growth of TiO2 Islands on Ferroelectric PbTiO3 Crystals to Boost Photocatalytic Activity. Joule, 2018, 2, 1095-1107.	11.7	113
231	Synthesis of rutile–anatase core–shell structured TiO2 for photocatalysis. Journal of Materials Chemistry, 2009, 19, 6590.	6.7	112
232	Sulfur doped anatase TiO2 single crystals with a high percentage of {0 0 1} facets. Journal of Colloid and Interface Science, 2010, 349, 477-483.	5.0	112
233	A Ta-TaS2 monolith catalyst with robust and metallic interface for superior hydrogen evolution. Nature Communications, 2021, 12, 6051.	5.8	112
234	Chemical Vapor Deposition Growth of Two-Dimensional Compound Materials: Controllability, Material Quality, and Growth Mechanism. Accounts of Materials Research, 2021, 2, 36-47.	5.9	111

#	Article	IF	CITATIONS
235	Strongly Coupled High-Quality Graphene/2D Superconducting Mo ₂ C Vertical Heterostructures with Aligned Orientation. ACS Nano, 2017, 11, 5906-5914.	7.3	110
236	High Reversible Lithium Storage Capacity and Structural Changes of Fe ₂ O ₃ Nanoparticles Confined inside Carbon Nanotubes. Advanced Energy Materials, 2016, 6, 1501755.	10.2	109
237	Anatase TiO ₂ Crystal Facet Growth: Mechanistic Role of Hydrofluoric Acid and Photoelectrocatalytic Activity. ACS Applied Materials & Interfaces, 2011, 3, 2472-2478.	4.0	108
238	Efficient Reversible Conversion between MoS ₂ and Mo/Na ₂ S Enabled by Graphene‣upported Single Atom Catalysts. Advanced Materials, 2021, 33, e2007090.	11.1	108
239	Challenges and development of lithium-ion batteries for low temperature environments. ETransportation, 2022, 11, 100145.	6.8	108
240	High-performance dual-gate carbon nanotube FETs with 40-nm gate length. IEEE Electron Device Letters, 2005, 26, 823-825.	2.2	107
241	TiO ₂ films with oriented anatase {001} facets and their photoelectrochemical behavior as CdS nanoparticle sensitized photoanodes. Journal of Materials Chemistry, 2011, 21, 869-873.	6.7	107
242	Dualâ€Phasic Carbon with Co Single Atoms and Nanoparticles as a Bifunctional Oxygen Electrocatalyst for Rechargeable Zn–Air Batteries. Advanced Functional Materials, 2021, 31, 2103360.	7.8	107
243	A General Singleâ€Source Route for the Preparation of Hollow Nanoporous Metal Oxide Structures. Angewandte Chemie - International Edition, 2009, 48, 7048-7051.	7.2	106
244	Unsaturated Single Atoms on Monolayer Transition Metal Dichalcogenides for Ultrafast Hydrogen Evolution. ACS Nano, 2020, 14, 767-776.	7.3	106
245	Grapheneâ€Supported Atomically Dispersed Metals as Bifunctional Catalysts for Nextâ€Generation Batteries Based on Conversion Reactions. Advanced Materials, 2022, 34, e2105812.	11.1	106
246	The morphology and thermal properties of multi-walled carbon nanotube and poly(hydroxybutyrate-co-hydroxyvalerate) composite. Polymer International, 2004, 53, 1479-1484.	1.6	105
247	Electrochemical performance of pyrolytic carbon-coated natural graphite spheres. Carbon, 2006, 44, 2212-2218.	5.4	105
248	Lithiation of Silicon Nanoparticles Confined in Carbon Nanotubes. ACS Nano, 2015, 9, 5063-5071.	7.3	105
249	The role of crystal phase in determining photocatalytic activity of nitrogen doped TiO2. Journal of Colloid and Interface Science, 2009, 329, 331-338.	5.0	104
250	NiPS ₃ Nanosheet–Graphene Composites as Highly Efficient Electrocatalysts for Oxygen Evolution Reaction. ACS Nano, 2018, 12, 5297-5305.	7.3	104
251	A nonflammable electrolyte for ultrahigh-voltage (4.8 V-class) Li NCM811 cells with a wide temperature range of 100 °C. Energy and Environmental Science, 2022, 15, 2435-2444.	15.6	104
252	Electrochemical Hydrogen Storage Behavior of Ropes of Aligned Single-Walled Carbon Nanotubes. Nano Letters, 2002, 2, 503-506.	4.5	103

#	Article	IF	CITATIONS
253	Increasing the electrical conductivity of carbon nanotube/polymer composites by using weak nanotube–polymer interactions. Carbon, 2010, 48, 3551-3558.	5.4	103
254	N-doped carbon nanotubes containing a high concentration of single iron atoms for efficient oxygen reduction. NPG Asia Materials, 2018, 10, e461-e461.	3.8	103
255	Effects of SWNT and Metallic Catalyst on Hydrogen Absorption/Desorption Performance of MgH2. Journal of Physical Chemistry B, 2005, 109, 22217-22221.	1.2	102
256	Frequency response characteristic of single-walled carbon nanotubes as supercapacitor electrode material. Applied Physics Letters, 2008, 92, .	1.5	102
257	Cadmium-containing quantum dots: properties, applications, and toxicity. Applied Microbiology and Biotechnology, 2017, 101, 2713-2733.	1.7	102
258	A Durable and Efficient Electrocatalyst for Saline Water Splitting with Current Density Exceeding 2000ÂmAÂcm ^{â^'2} . Advanced Functional Materials, 2021, 31, 2010367.	7.8	102
259	Carbon nanotubes for clean energy applications. Journal Physics D: Applied Physics, 2005, 38, R231-R252.	1.3	101
260	Thermodynamically tuning LiBH4 by fluorine anion doping for hydrogen storage: A density functional study. Chemical Physics Letters, 2008, 450, 318-321.	1.2	101
261	High-Quality, Highly Concentrated Semiconducting Single-Wall Carbon Nanotubes for Use in Field Effect Transistors and Biosensors. ACS Nano, 2013, 7, 6831-6839.	7.3	101
262	Unique Domain Structure of Two-Dimensional α-Mo ₂ C Superconducting Crystals. Nano Letters, 2016, 16, 4243-4250.	4.5	101
263	Vertical Chemical Vapor Deposition Growth of Highly Uniform 2D Transition Metal Dichalcogenides. ACS Nano, 2020, 14, 4646-4653.	7.3	101
264	Repeated Growth–Etching–Regrowth for Large-Area Defect-Free Single-Crystal Graphene by Chemical Vapor Deposition. ACS Nano, 2014, 8, 12806-12813.	7.3	100
265	Selective deposition of redox co-catalyst(s) to improve the photocatalytic activity of single-domain ferroelectric PbTiO ₃ nanoplates. Chemical Communications, 2014, 50, 10416.	2.2	100
266	A selectively exposed crystal facet-engineered TiO2 thin film photoanode for the higher performance of the photoelectrochemical water splitting reaction. Energy and Environmental Science, 2015, 8, 3646-3653.	15.6	100
267	A flexible cotton-derived carbon sponge for high-performance capacitive deionization. Carbon, 2016, 101, 1-8.	5.4	100
268	Mass production of 2D materials by intermediate-assisted grinding exfoliation. National Science Review, 2020, 7, 324-332.	4.6	100
269	Visibleâ€Lightâ€Responsive βâ€Rhombohedral Boron Photocatalysts. Angewandte Chemie - International Edition, 2013, 52, 6242-6245.	7.2	99
270	Mesopore-Aspect-Ratio Dependence of Ion Transport in Rodtype Ordered Mesoporous Carbon. Journal of Physical Chemistry C, 2008, 112, 9950-9955.	1.5	98

#	Article	IF	CITATIONS
271	Co3O4 mesoporous nanostructures@graphene membrane as an integrated anode for long-life lithium-ion batteries. Journal of Power Sources, 2014, 255, 52-58.	4.0	98
272	Aligned Titania Nanotubes as an Intercalation Anode Material for Hybrid Electrochemical Energy Storage. Advanced Functional Materials, 2008, 18, 3787-3793.	7.8	97
273	Carbon nanotube encapsulated in nitrogen and phosphorus co-doped carbon as a bifunctional electrocatalyst for oxygen reduction and evolution reactions. Carbon, 2018, 139, 156-163.	5.4	97
274	ZnS Branched Architectures as Optoelectronic Devices and Field Emitters. Advanced Materials, 2010, 22, 2376-2380.	11.1	96
275	Bulk growth of mono- to few-layer graphene on nickel particles by chemical vapor deposition from methane. Carbon, 2010, 48, 3543-3550.	5.4	96
276	Charge delivery goes the distance. Science, 2017, 356, 582-583.	6.0	96
277	Mg-Based Nanocomposites with High Capacity and Fast Kinetics for Hydrogen Storage. Journal of Physical Chemistry B, 2006, 110, 11697-11703.	1.2	95
278	Improved capacitance of SBA-15 templated mesoporous carbons after modification with nitric acid oxidation. New Carbon Materials, 2007, 22, 307-314.	2.9	95
279	Nitrogen-doped titania nanosheets towards visible light response. Chemical Communications, 2009, , 1383.	2.2	95
280	Ionâ€Dipole Chemistry Drives Rapid Evolution of Li Ions Solvation Sheath in Lowâ€Temperature Li Batteries. Advanced Energy Materials, 2021, 11, 2100935.	10.2	95
281	Visibleâ€Lightâ€Active Elemental Photocatalysts. ChemPhysChem, 2013, 14, 885-892.	1.0	93
282	Designing Electrophilic and Nucleophilic Dual Centers in the ReS ₂ Plane toward Efficient Bifunctional Catalysts for Li-CO ₂ Batteries. Journal of the American Chemical Society, 2022, 144, 3106-3116.	6.6	93
283	Reliable liquid electrolytes for lithium metal batteries. Energy Storage Materials, 2020, 30, 113-129.	9.5	92
284	Field emission from AlN nanorod array. Applied Physics Letters, 2005, 86, 153104.	1.5	91
285	New Insight into the Solid Electrolyte Interphase with Use of a Focused Ion Beam. Journal of Physical Chemistry B, 2005, 109, 22205-22211.	1.2	89
286	Facile and Controlled Synthesis of 3D Nanorods-Based Urchinlike and Nanosheets-Based Flowerlike Cobalt Basic Salt Nanostructures. Journal of Physical Chemistry C, 2007, 111, 3848-3852.	1.5	88
287	Diameter-Selective Growth of Single-Walled Carbon Nanotubes with High Quality by Floating Catalyst Method. ACS Nano, 2008, 2, 1722-1728.	7.3	88
288	Quantifying the Volumetric Performance Metrics of Supercapacitors. Advanced Energy Materials, 2019, 9, 1900079.	10.2	88

#	Article	IF	CITATIONS
289	An array of Eiffel-tower-shape AlN nanotips and its field emission properties. Applied Physics Letters, 2005, 86, 233104.	1.5	87
290	Surface and Interference Coenhanced Raman Scattering of Graphene. ACS Nano, 2009, 3, 933-939.	7.3	87
291	Direct and green repairing of degraded LiCoO2 for reuse in lithium-ion batteries. National Science Review, 2022, 9, .	4.6	85
292	Surface modification of single-walled carbon nanotubes with polyethylene viain situ Ziegler-Natta polymerization. Journal of Applied Polymer Science, 2004, 92, 3697-3700.	1.3	84
293	Exploration of the Nature of Active Ti Species in Metallic Ti-Doped NaAlH4. Journal of Physical Chemistry B, 2005, 109, 20131-20136.	1.2	84
294	Carbon nanotubes: controlled growth and application. Materials Today, 2013, 16, 19-28.	8.3	84
295	Tuning the Electrical and Optical Properties of Graphene by Ozone Treatment for Patterning Monolithic Transparent Electrodes. ACS Nano, 2013, 7, 4233-4241.	7.3	84
296	High-rate lithium storage of anatase TiO2 crystals doped with both nitrogen and sulfur. Chemical Communications, 2013, 49, 3461.	2.2	84
297	A gradient bi-functional graphene-based modified electrode for vanadium redox flow batteries. Energy Storage Materials, 2018, 13, 66-71.	9.5	84
298	Functional anion concept: effect of fluorine anion on hydrogen storage of sodium alanate. Physical Chemistry Chemical Physics, 2007, 9, 1499-1502.	1.3	83
299	Free-Standing Highly Conductive Transparent Ultrathin Single-Walled Carbon Nanotube Films. Journal of the American Chemical Society, 2010, 132, 16581-16586.	6.6	83
300	Armoring Graphene Cathodes for Highâ€Rate and Long‣ife Lithium Ion Supercapacitors. Advanced Energy Materials, 2016, 6, 1502064.	10.2	83
301	Strategies for Modifying TiO ₂ Based Electron Transport Layers to Boost Perovskite Solar Cells. ACS Sustainable Chemistry and Engineering, 2019, 7, 4586-4618.	3.2	83
302	Hydrogen sorption kinetics of MgH2 catalyzed with NbF5. Journal of Alloys and Compounds, 2008, 453, 138-142.	2.8	82
303	Tension–tension fatigue behavior of unidirectional single-walled carbon nanotube reinforced epoxy composite. Carbon, 2003, 41, 2177-2179.	5.4	81
304	Preparation of Metallic Single-Wall Carbon Nanotubes by Selective Etching. ACS Nano, 2014, 8, 7156-7162.	7.3	81
305	Comprehensive evaluation of the cytotoxicity of CdSe/ZnS quantum dots in Phanerochaete chrysosporium by cellular uptake and oxidative stress. Environmental Science: Nano, 2017, 4, 2018-2029.	2.2	81
306	Synthesis and dye separation performance of ferromagnetic hierarchical porous carbon. Carbon, 2008, 46, 1593-1599.	5.4	80

#	Article	IF	CITATIONS
307	Hydrogen sorption kinetics of MgH2 catalyzed with titanium compounds. International Journal of Hydrogen Energy, 2010, 35, 3046-3050.	3.8	80
308	Tween 80 surfactant-enhanced bioremediation: toward a solution to the soil contamination by hydrophobic organic compounds. Critical Reviews in Biotechnology, 2018, 38, 17-30.	5.1	80
309	The fabrication of a carbon nanotube transparent conductive film by electrophoretic deposition and hot-pressing transfer. Nanotechnology, 2009, 20, 235707.	1.3	79
310	Greatly Enhanced Electronic Conduction and Lithium Storage of Faceted TiO ₂ Crystals Supported on Metallic Substrates by Tuning Crystallographic Orientation of TiO ₂ . Advanced Materials, 2015, 27, 3507-3512.	11.1	79
311	Chitosan-wrapped gold nanoparticles for hydrogen-bonding recognition and colorimetric determination of the antibiotic kanamycin. Mikrochimica Acta, 2017, 184, 2097-2105.	2.5	79
312	Reduced graphene oxide/metal oxide nanoparticles composite membranes for highly efficient molecular separation. Journal of Materials Science and Technology, 2018, 34, 1481-1486.	5.6	79
313	Computational design and property predictions for two-dimensional nanostructures. Materials Today, 2018, 21, 391-418.	8.3	78
314	Bi-Cation Electrolyte for a 1.7 V Aqueous Zn Ion Battery. ACS Applied Materials & Interfaces, 2020, 12, 13790-13796.	4.0	78
315	High-purity single-wall carbon nanotubes synthesized from coal by arc discharge. Carbon, 2003, 41, 2170-2173.	5.4	77
316	Edge phonon state of mono- and few-layer graphene nanoribbons observed by surface and interference co-enhanced Raman spectroscopy. Physical Review B, 2010, 81, .	1.1	77
317	Controlled Growth of Semiconducting and Metallic Single-Wall Carbon Nanotubes. Journal of the American Chemical Society, 2016, 138, 6690-6698.	6.6	77
318	Quantitative Analysis of Temperature Dependence of Raman shift of monolayer WS2. Scientific Reports, 2016, 6, 32236.	1.6	77
319	Growth Velocity and Direct Length-Sorted Growth of Short Single-Walled Carbon Nanotubes by a Metal-Catalyst-Free Chemical Vapor Deposition Process. ACS Nano, 2009, 3, 3421-3430.	7.3	76
320	High temperature selective growth of single-walled carbon nanotubes with a narrow chirality distribution from a CoPt bimetallic catalyst. Chemical Communications, 2012, 48, 2409.	2.2	75
321	Growth of semiconducting single-wall carbon nanotubes with a narrow band-gap distribution. Nature Communications, 2016, 7, 11160.	5.8	75
322	Thermal expansion of a composite of single-walled carbon nanotubes and nanocrystalline aluminum. Carbon, 2004, 42, 3260-3262.	5.4	74
323	Structure and thermal expansion of multi-walled carbon nanotubes before and after high temperature treatment. Journal Physics D: Applied Physics, 2005, 38, 4302-4307.	1.3	74
324	Hierarchically porous Fe-N-doped carbon nanotubes as efficient electrocatalyst for oxygen reduction. Carbon, 2016, 109, 632-639.	5.4	74

#	Article	IF	CITATIONS
325	Engineering Two-Dimensional Materials and Their Heterostructures as High-Performance Electrocatalysts. Electrochemical Energy Reviews, 2019, 2, 373-394.	13.1	74
326	Synthesis and Photoelectrochemical Property of Urchin-like Zn/ZnO Coreâ^'Shell Structures. Journal of Physical Chemistry C, 2009, 113, 11035-11040.	1.5	73
327	The examination of graphene oxide for rechargeable lithium storage as a novel cathode material. Journal of Materials Chemistry A, 2013, 1, 3607.	5.2	73
328	Towards the practical use of flexible lithium ion batteries. Energy Storage Materials, 2019, 23, 434-438.	9.5	73
329	Interstitial-boron solution strengthened WB3+ <i>x</i> . Applied Physics Letters, 2013, 103, .	1.5	72
330	Structure, Preparation, and Applications of 2D Materialâ€Based Metal–Semiconductor Heterostructures. Small Structures, 2021, 2, 2000093.	6.9	71
331	Engineering the Active Sites of Graphene Catalyst: From CO ₂ Activation to Activate Li-CO ₂ Batteries. ACS Nano, 2021, 15, 9841-9850.	7.3	71
332	High-Performance Lithium Metal Batteries with a Wide Operating Temperature Range in Carbonate Electrolyte by Manipulating Interfacial Chemistry. ACS Energy Letters, 2021, 6, 3170-3179.	8.8	71
333	Facile Fabrication of Anatase TiO ₂ Microspheres on Solid Substrates and Surface Crystal Facet Transformation from {001} to {101}. Chemistry - A European Journal, 2011, 17, 5949-5957.	1.7	70
334	A LiF Nanoparticleâ€Modified Graphene Electrode for Highâ€Power and Highâ€Energy Lithium Ion Batteries. Advanced Functional Materials, 2012, 22, 3290-3297.	7.8	70
335	Nanosize SnO2 confined in the porous shells of carbon cages for kinetically efficient and long-term lithium storage. Nanoscale, 2013, 5, 1576.	2.8	70
336	Fluorination-assisted preparation of self-supporting single-atom Fe-N-doped single-wall carbon nanotube film as bifunctional oxygen electrode for rechargeable Zn-Air batteries. Applied Catalysis B: Environmental, 2021, 294, 120239.	10.8	70
337	Preparation, morphology, and microstructure of diameter-controllable vapor-grown carbon nanofibers. Journal of Materials Research, 1998, 13, 2342-2346.	1.2	69
338	Synthesis of different magnetic carbon nanostructures by the pyrolysis of ferrocene at different sublimation temperatures. Carbon, 2008, 46, 1892-1902.	5.4	69
339	Improved Reversible Dehydrogenation of Lithium Borohydride by Milling with As-Prepared Single-Walled Carbon Nanotubes. Journal of Physical Chemistry C, 2008, 112, 17023-17029.	1.5	69
340	Hollow carbon cage with nanocapsules of graphitic shell/nickel core as an anode material for high rate lithium ion batteries. Journal of Materials Chemistry, 2012, 22, 11252.	6.7	69
341	Magnetotransport Properties in High-Quality Ultrathin Two-Dimensional Superconducting Mo ₂ C Crystals. ACS Nano, 2016, 10, 4504-4510.	7.3	69
342	Micro-mechanical properties and morphological observation on fracture surfaces of carbon nanotube composites pre-treated at different temperatures. Composites Science and Technology, 2003, 63, 1161-1164.	3.8	68

#	Article	IF	CITATIONS
343	Drastically enhanced photocatalytic activity in nitrogen doped mesoporous TiO2 with abundant surface states. Journal of Colloid and Interface Science, 2009, 334, 171-175.	5.0	68
344	Crystallographic Tailoring of Graphene by Nonmetal SiO _{<i>x</i>} Nanoparticles. Journal of the American Chemical Society, 2009, 131, 13934-13936.	6.6	68
345	Reduced graphene oxide with a highly restored ï€-conjugated structure for inkjet printing and its use in all-carbon transistors. Nano Research, 2013, 6, 842-852.	5.8	68
346	Effects of edge on graphene plasmons as revealed by infrared nanoimaging. Light: Science and Applications, 2017, 6, e16204-e16204.	7.7	68
347	Transfer Methods of Graphene from Metal Substrates: A Review. Small Methods, 2019, 3, 1900049.	4.6	67
348	A Nanosheet Array of Cu ₂ Se Intercalation Compound with Expanded Interlayer Space for Sodium Ion Storage. Advanced Energy Materials, 2020, 10, 2000666.	10.2	67
349	Influence of ferrocene/benzene mole ratio on the synthesis of carbon nanostructures. Chemical Physics Letters, 2003, 376, 83-89.	1.2	65
350	Improving hydrogen sorption kinetics of MgH2 by mechanical milling with TiF3. Journal of Alloys and Compounds, 2007, 432, L1-L4.	2.8	65
351	Bulk Storage Capacity of Hydrogen in Purified Multiwalled Carbon Nanotubes. Journal of Physical Chemistry B, 2002, 106, 963-966.	1.2	64
352	Synthesis and characterization of double-walled carbon nanotubes from multi-walled carbon nanotubes by hydrogen-arc discharge. Carbon, 2005, 43, 623-629.	5.4	64
353	Synthesis and photoluminescence of tetrapod ZnO nanostructures. Chemical Physics Letters, 2007, 434, 301-305.	1.2	64
354	Graphitization Behavior of Wood Ceramics and Bamboo Ceramics as Determined by X-Ray Diffraction. Journal of Porous Materials, 1999, 6, 233-237.	1.3	63
355	Volumetric hydrogen storage in single-walled carbon nanotubes. Applied Physics Letters, 2002, 80, 2389-2391.	1.5	63
356	TiO2/graphene sandwich paper as an anisotropic electrode for high rate lithium ion batteries. Nanoscale, 2013, 5, 7780.	2.8	63
357	Localized polyselenides in a graphene-coated polymer separator for high rate and ultralong life lithium–selenium batteries. Chemical Communications, 2015, 51, 3667-3670.	2.2	63
358	Continuous Fabrication of Meterâ€Scale Singleâ€Wall Carbon Nanotube Films and their Use in Flexible and Transparent Integrated Circuits. Advanced Materials, 2018, 30, e1802057.	11.1	63
359	Status and prospects of porous graphene networks for lithium–sulfur batteries. Materials Horizons, 2020, 7, 2487-2518.	6.4	63
360	Single-atom catalysts for metal-sulfur batteries: Current progress and future perspectives. Journal of Energy Chemistry, 2021, 54, 452-466.	7.1	63

HUI-MING CHENG

#	Article	IF	CITATIONS
361	Synthesis of Carbon Nanotubes by Floating Catalyst Chemical Vapor Deposition and Their Applications. Advanced Functional Materials, 2022, 32, 2108541.	7.8	63
362	Microwave Electromagnetic Characteristics of a Microcoiled Carbon Fibers/paraffin Wax Composite in Ku Band. Journal of Materials Research, 2002, 17, 1232-1236.	1.2	62
363	Van der Waals interactions between two parallel infinitely long single-walled nanotubes. Chemical Physics Letters, 2005, 403, 343-346.	1.2	62
364	Urchin-like nano/micro hybrid anode materials for lithium ion battery. Carbon, 2006, 44, 2778-2784.	5.4	62
365	The Effect of Sulfur on the Structure of Carbon Nanotubes Produced by a Floating Catalyst Method. Journal of Nanoscience and Nanotechnology, 2006, 6, 1339-1345.	0.9	62
366	The doping of reduced graphene oxide with nitrogen and its effect on the quenching of the material's photoluminescence. Carbon, 2012, 50, 5286-5291.	5.4	62
367	The application of Zeolitic imidazolate frameworks (ZIFs) and their derivatives based materials for photocatalytic hydrogen evolution and pollutants treatment. Chemical Engineering Journal, 2021, 417, 127914.	6.6	62
368	Crystallinity-dependent substitutional nitrogen doping in ZnO and its improved visible light photocatalytic activity. Journal of Colloid and Interface Science, 2013, 400, 18-23.	5.0	61
369	An overview on nitride and nitrogen-doped photocatalysts for energy and environmental applications. Composites Part B: Engineering, 2019, 172, 704-723.	5.9	61
370	Homogeneous Doping of Substitutional Nitrogen/Carbon in TiO ₂ Plates for Visible Light Photocatalytic Water Oxidation. Advanced Functional Materials, 2019, 29, 1901943.	7.8	61
371	Efficient and stable photocatalytic H2 evolution from water splitting by (Cd0.8Zn0.2)S nanorods. Electrochemistry Communications, 2009, 11, 1174-1178.	2.3	60
372	Triangle defect states of hexagonal boron nitride atomic layer: Density functional theory calculations. Physical Review B, 2010, 81, .	1.1	60
373	Perfect proton selectivity in ion transport through two-dimensional crystals. Nature Communications, 2019, 10, 4243.	5.8	60
374	Synthesis and applications of three-dimensional graphene network structures. Materials Today Nano, 2019, 5, 100027.	2.3	60
375	A highly active and durable electrocatalyst for large current density hydrogen evolution reaction. Science Bulletin, 2020, 65, 123-130.	4.3	58
376	Glue-assisted grinding exfoliation of large-size 2D materials for insulating thermal conduction and large-current-density hydrogen evolution. Materials Today, 2021, 51, 145-154.	8.3	58
377	Structure and hydrogen storage property of ball-milled LiNH2/MgH2LiNH2/MgH2 mixture. International Journal of Hydrogen Energy, 2006, 31, 1236-1240.	3.8	57
378	Enhanced hydrogen storage properties of MgH2 co-catalyzed with NbF5 and single-walled carbon nanotubes. Scripta Materialia, 2007, 56, 765-768.	2.6	57

#	Article	IF	CITATIONS
379	Direct synthesis of carbon nanotubes decorated with size-controllable Fe nanoparticles encapsulated by graphitic layers. Carbon, 2008, 46, 1417-1423.	5.4	57
380	Second Time-Scale Synthesis of High-Quality Graphite Films by Quenching for Effective Electromagnetic Interference Shielding. ACS Nano, 2020, 14, 3121-3128.	7.3	57
381	A TEM study of microstructure of carbon fiber/polycarbosilane-derived SiC composites. Carbon, 1999, 37, 2057-2062.	5.4	56
382	Semiconducting properties of cup-stacked carbon nanotubes. Carbon, 2009, 47, 731-736.	5.4	56
383	Nonstoichiometric rutile TiO2 photoelectrodes for improved photoelectrochemical water splitting. Chemical Communications, 2013, 49, 6191.	2.2	56
384	Carbon nanotube-linked hollow carbon nanospheres doped with iron and nitrogen as single-atom catalysts for the oxygen reduction reaction in acidic solutions. Journal of Materials Chemistry A, 2019, 7, 14478-14482.	5.2	56
385	A Freestanding Singleâ€Wall Carbon Nanotube Film Decorated with Nâ€Đoped Carbonâ€Encapsulated Ni Nanoparticles as a Bifunctional Electrocatalyst for Overall Water Splitting. Advanced Science, 2019, 6, 1802177.	5.6	56
386	Atomicâ€Scale Design of Anode Materials for Alkali Metal (Li/Na/K)â€Ion Batteries: Progress and Perspectives. Advanced Energy Materials, 2022, 12, .	10.2	56
387	Preparation of single-crystal α-MnO2 nanorods and nanoneedles from aqueous solution. Journal of Alloys and Compounds, 2005, 397, 282-285.	2.8	55
388	3D Aperiodic Hierarchical Porous Graphitic Carbon Material for Highâ€Rate Electrochemical Capacitive Energy Storage. Angewandte Chemie - International Edition, 2009, 48, 1525-1525.	7.2	55
389	Synthesis of mesoporous single crystal rutile TiO2 with improved photocatalytic and photoelectrochemical activities. Chemical Communications, 2013, 49, 11770.	2.2	55
390	A nitrogen-doped mesoporous carbon containing an embedded network of carbon nanotubes as a highly efficient catalyst for the oxygen reduction reaction. Nanoscale, 2015, 7, 19201-19206.	2.8	55
391	An integrated electrode/separator with nitrogen and nickel functionalized carbon hybrids for advanced lithium/polysulfide batteries. Carbon, 2016, 109, 719-726.	5.4	55
392	Sustainable hydrogen production by molybdenum carbide-based efficient photocatalysts: From properties to mechanism. Advances in Colloid and Interface Science, 2020, 279, 102144.	7.0	55
393	An in-situ solidification strategy to block polysulfides in Lithium-Sulfur batteries. Energy Storage Materials, 2021, 37, 224-232.	9.5	55
394	Multifunctional fabrics of carbon nanotube fibers. Journal of Materials Chemistry A, 2019, 7, 8790-8797.	5.2	54
395	Dualâ€Additive Assisted Chemical Vapor Deposition for the Growth of Mnâ€Doped 2D MoS ₂ with Tunable Electronic Properties. Small, 2020, 16, e1903181.	5.2	54
396	Modulating Electronic Structure of Monolayer Transition Metal Dichalcogenides by Substitutional Nbâ€Doping. Advanced Functional Materials, 2021, 31, 2006941.	7.8	54

#	Article	IF	CITATIONS
397	The role of NH3 atmosphere in preparing nitrogen-doped TiO2 by mechanochemical reaction. Journal of Solid State Chemistry, 2006, 179, 331-335.	1.4	53
398	Doping Concentration Modulation in Vanadium-Doped Monolayer Molybdenum Disulfide for Synaptic Transistors. ACS Nano, 2021, 15, 7340-7347.	7.3	53
399	Boron oxynitride nanoclusters on tungsten trioxide as a metal-free cocatalyst for photocatalytic oxygen evolution from water splitting. Nanoscale, 2012, 4, 1267.	2.8	52
400	Ablation and mechanical behavior of a sandwich-structured composite with an inner layer of Cf/SiC between two outer layers of Cf/SiC–ZrB2–ZrC. Corrosion Science, 2014, 80, 154-163.	3.0	52
401	Structural Changes in Iron Oxide and Gold Catalysts during Nucleation of Carbon Nanotubes Studied by <i>In Situ</i> Transmission Electron Microscopy. ACS Nano, 2014, 8, 292-301.	7.3	52
402	Electrochemical DNA sensing strategy based on strengthening electronic conduction and a signal amplifier carrier of nanoAu/MCN composited nanomaterials for sensitive lead detection. Environmental Science: Nano, 2016, 3, 1504-1509.	2.2	52
403	Boosting photoelectrochemical water splitting performance of Ta3N5 nanorod array photoanodes by forming a dual co-catalyst shell. Nano Energy, 2019, 59, 683-688.	8.2	52
404	Ultralight carbon fiber felt reinforced monolithic carbon aerogel composites with excellent thermal insulation performance. Carbon, 2021, 183, 525-529.	5.4	52
405	Toward an Understanding of the Reversible Li-CO ₂ Batteries over Metal–N ₄ -Functionalized Graphene Electrocatalysts. ACS Nano, 2022, 16, 1523-1532.	7.3	52
406	Electronic structure adjustment of lithium sulfide by a single-atom copper catalyst toward high-rate lithium-sulfur batteries. Energy Storage Materials, 2022, 51, 890-899.	9.5	52
407	The influence of preparation parameters on the mass production of vapor-grown carbon nanofibers. Carbon, 2000, 38, 789-795.	5.4	51
408	Micro-hardness and Flexural Properties of Randomly-oriented Carbon Nanotube Composites. Journal of Composite Materials, 2003, 37, 365-376.	1.2	51
409	Pore structures of multi-walled carbon nanotubes activated by air, CO2 and KOH. Journal of Porous Materials, 2006, 13, 141-146.	1.3	51
410	Additiveâ€Free Dispersion of Singleâ€Walled Carbon Nanotubes and Its Application for Transparent Conductive Films. Advanced Functional Materials, 2011, 21, 2330-2337.	7.8	51
411	High-performance single-wall carbon nanotube transparent conductive films. Journal of Materials Science and Technology, 2019, 35, 2447-2462.	5.6	51
412	Precise Identification of the Active Phase of Cobalt Catalyst for Carbon Nanotube Growth by <i>In Situ</i> Transmission Electron Microscopy. ACS Nano, 2020, 14, 16823-16831.	7.3	51
413	Synthesis and High Thermal Stability of Double-Walled Carbon Nanotubes Using Nickel Formate Dihydrate as Catalyst Precursor. Journal of Physical Chemistry C, 2007, 111, 5006-5013.	1.5	50
414	Controllable Synthesis of Vertically Aligned pâ€Type GaN Nanorod Arrays on nâ€Type Si Substrates for Heterojunction Diodes. Advanced Functional Materials, 2008, 18, 3515-3522.	7.8	50

HUI-MING CHENG

#	Article	IF	CITATIONS
415	Selective removal of metallic single-walled carbon nanotubes by combined in situ and post-synthesis oxidation. Carbon, 2010, 48, 2941-2947.	5.4	50
416	Superiority of Graphene over Polymer Coatings for Prevention of Microbially Induced Corrosion. Scientific Reports, 2015, 5, 13858.	1.6	50
417	Structural Control of Graphene-Based Materials for Unprecedented Performance. ACS Nano, 2018, 12, 5085-5092.	7.3	50
418	Surface and interface engineering of two-dimensional bismuth-based photocatalysts for ambient molecule activation. Journal of Materials Chemistry A, 2021, 9, 196-233.	5.2	50
419	Dissolution–Precipitation Dynamics in Ester Electrolyte for High-Stability Lithium Metal Batteries. ACS Energy Letters, 0, , 1413-1421.	8.8	50
420	Graphene oxide/graphene vertical heterostructure electrodes for highly efficient and flexible organic light emitting diodes. Nanoscale, 2016, 8, 10714-10723.	2.8	49
421	Thermal characterization of single-wall carbon nanotube bundles using the self-heating 3ï‰ technique. Journal of Applied Physics, 2006, 100, 124314.	1.1	48
422	Synthesis and photoluminescent property of AlN nanobelt array. Diamond and Related Materials, 2007, 16, 537-541.	1.8	48
423	Growth, Cathodoluminescence and Field Emission of ZnS Tetrapod Treeâ€like Heterostructures. Advanced Functional Materials, 2008, 18, 3063-3069.	7.8	48
424	Visualizing the roles of graphene for excellent lithium storage. Journal of Materials Chemistry A, 2014, 2, 17808-17814.	5.2	48
425	Efficient adsorption of organic dyes on a flexible single-wall carbon nanotube film. Journal of Materials Chemistry A, 2016, 4, 1191-1194.	5.2	48
426	Noninvasively Modifying Band Structures of Wideâ€Bandgap Metal Oxides to Boost Photocatalytic Activity. Advanced Materials, 2018, 30, e1706259.	11.1	48
427	A MnO2 nanosheet/single-wall carbon nanotube hybrid fiber for wearable solid-state supercapacitors. Carbon, 2018, 140, 634-643.	5.4	48
428	Porous Graphene Materials: The Chemistry and Promising Applications of Graphene and Porous Graphene Materials (Adv. Funct. Mater. 41/2020). Advanced Functional Materials, 2020, 30, 2070275.	7.8	48
429	Megamerger of MOFs and g-C ₃ N ₄ for energy and environment applications: upgrading the framework stability and performance. Journal of Materials Chemistry A, 2020, 8, 17883-17906.	5.2	48
430	A Flexible Carbon Nanotube Senâ€Memory Device. Advanced Materials, 2020, 32, e1907288.	11.1	48
431	Axial Young's modulus prediction of single-walled carbon nanotube arrays with diameters from nanometer to meter scales. Applied Physics Letters, 2005, 87, 193101.	1.5	47
432	Field Emission and Cathodoluminescence of ZnS Hexagonal Pyramids of Zinc Blende Structured Single Crystals. Advanced Functional Materials, 2009, 19, 484-490.	7.8	47

#	Article	IF	CITATIONS
433	Tunable p-Type Conductivity and Transport Properties of AlN Nanowires <i>via</i> Mg Doping. ACS Nano, 2011, 5, 3591-3598.	7.3	47
434	Combined removal of di(2-ethylhexyl)phthalate (DEHP) and Pb(<scp>ii</scp>) by using a cutinase loaded nanoporous gold-polyethyleneimine adsorbent. RSC Advances, 2014, 4, 55511-55518.	1.7	47
435	Smart Materials and Design toward Safe and Durable Lithium Ion Batteries. Small Methods, 2019, 3, 1900323.	4.6	47
436	Fatigue failure mechanisms of single-walled carbon nanotube ropes embedded in epoxy. Applied Physics Letters, 2004, 84, 2811-2813.	1.5	46
437	Synthesis of Tin (II or IV) Oxide Coated Multiwall Carbon Nanotubes with Controlled Morphology. Journal of Physical Chemistry C, 2008, 112, 5790-5794.	1.5	46
438	Substitutional Carbonâ€Modified Anatase TiO ₂ Decahedral Plates Directly Derived from Titanium Oxalate Crystals via Topotactic Transition. Advanced Materials, 2018, 30, e1705999.	11.1	46
439	Long-term oxidation behaviors of C/SiC composites with a SiC/UHTC/SiC three-layer coating in a wide temperature range. Corrosion Science, 2019, 147, 1-8.	3.0	46
440	Monolayer carbon-encapsulated Mo-doped Ni nanoparticles anchored on single-wall carbon nanotube film for total water splitting. Applied Catalysis B: Environmental, 2020, 269, 118823.	10.8	46
441	Aligned Double-Walled Carbon Nanotube Long Ropes with a Narrow Diameter Distribution. Journal of Physical Chemistry B, 2005, 109, 7169-7173.	1.2	45
442	Evidence for, and an Understanding of, the Initial Nucleation of Carbon Nanotubes Produced by a Floating Catalyst Method. Journal of Physical Chemistry B, 2006, 110, 16941-16946.	1.2	45
443	Boosting efficiency and stability of perovskite solar cells with nickel phthalocyanine as a low-cost hole transporting layer material. Journal of Materials Science and Technology, 2018, 34, 1474-1480.	5.6	45
444	Silicaâ€Mediated Formation of Nickel Sulfide Nanosheets on CNT Films for Versatile Energy Storage. Small, 2019, 15, e1805064.	5.2	45
445	Fabrication of Large Aerogel-Like Carbon/Carbon Composites with Excellent Load-Bearing Capacity and Thermal-Insulating Performance at 1800 °C. ACS Nano, 2022, 16, 6565-6577.	7.3	45
446	Tailoring the diameters of vapor-grown carbon nanofibers. Carbon, 2000, 38, 921-927.	5.4	44
447	Structure and morphology of microporous carbon membrane materials derived from poly(phthalazinone ether sulfone ketone). Microporous and Mesoporous Materials, 2006, 96, 79-83.	2.2	44
448	In situ formation and rapid decomposition of Ti(BH4)3 by mechanical milling LiBH4 with TiF3. Applied Physics Letters, 2009, 94, 044104.	1.5	44
449	Constructing a Metallic/Semiconducting TaB ₂ /Ta ₂ O ₅ Core/Shell Heterostructure for Photocatalytic Hydrogen Evolution. Advanced Energy Materials, 2014, 4, 1400057.	10.2	44
450	Graphene-based integrated electrodes for flexible lithium ion batteries. 2D Materials, 2015, 2, 024004.	2.0	44

#	Article	IF	CITATIONS
451	Combined biological removal of methylene blue from aqueous solutions using rice straw and Phanerochaete chrysosporium. Applied Microbiology and Biotechnology, 2015, 99, 5247-5256.	1.7	44
452	Synthesis and Electrochemical Lithium Storage Behavior of Carbon Nanotubes Filled with Iron Sulfide Nanoparticles. Advanced Science, 2016, 3, 1600113.	5.6	44
453	Lithiumâ€Sulfur Batteries: Metal–Organic Frameworks (MOFs)â€Derived Nitrogenâ€Doped Porous Carbon Anchored on Graphene with Multifunctional Effects for Lithium–Sulfur Batteries (Adv. Funct. Mater.) Tj ETQq1 I	1 0. 88431	.4 4g BT /Ove
454	Identification of active sites in nitrogen and sulfur co-doped carbon-based oxygen reduction catalysts. Carbon, 2019, 147, 303-311.	5.4	44
455	Field emission properties of macroscopic single-walled carbon nanotube strands. Applied Physics Letters, 2005, 86, 223114.	1.5	43
456	Long-term oxidation behavior of carbon/carbon composites with a SiC/B4C–B2O3–SiO2–Al2O3 coating at low and medium temperatures. Corrosion Science, 2015, 94, 452-458.	3.0	43
457	An Aluminum–Sulfur Battery with a Fast Kinetic Response. Angewandte Chemie, 2018, 130, 1916-1920.	1.6	43
458	Small-bundle single-wall carbon nanotubes for high-efficiency silicon heterojunction solar cells. Nano Energy, 2018, 50, 521-527.	8.2	43
459	Ultrafast growth of nanocrystalline graphene films by quenching and grain-size-dependent strength and bandgap opening. Nature Communications, 2019, 10, 4854.	5.8	43
460	Suppressing lithium dendrite formation by slowing its desolvation kinetics. Chemical Communications, 2019, 55, 13211-13214.	2.2	43
461	Interlayer epitaxy of wafer-scale high-quality uniform AB-stacked bilayer graphene films on liquid Pt3Si/solid Pt. Nature Communications, 2019, 10, 2809.	5.8	43
462	Carbon nanotube/silicon heterojunctions for photovoltaic applications. Nano Materials Science, 2019, 1, 156-172.	3.9	43
463	Vertically aligned carbon nanotube arrays as a thermal interface material. APL Materials, 2019, 7, .	2.2	43
464	Catalytically Enhanced Hydrogen Storage Properties of Mg(NH ₂) ₂ + 2LiH Material by Graphite-Supported Ru Nanoparticles. Journal of Physical Chemistry C, 2008, 112, 18280-18285.	1.5	42
465	Effect of carbonization atmosphere on the structure changes of PAN carbon membranes. Journal of Porous Materials, 2009, 16, 197-203.	1.3	42
466	Titania polymorphs derived from crystalline titanium diboride. CrystEngComm, 2009, 11, 2677.	1.3	42
467	Double-wall carbon nanotube transparent conductive films with excellent performance. Journal of Materials Chemistry A, 2014, 2, 1159-1164.	5.2	42
468	Synthesis and Application of Modified Zero-Valent Iron Nanoparticles for Removal of Hexavalent Chromium from Wastewater. Water, Air, and Soil Pollution, 2015, 226, 1.	1.1	42

#	Article	IF	CITATIONS
469	Electrochemical process of sulfur in carbon materials from electrode thickness to interlayer. Journal of Energy Chemistry, 2019, 31, 119-124.	7.1	42
470	Intercalation-Induced Conversion Reactions Give High-Capacity Potassium Storage. ACS Nano, 2020, 14, 14026-14035.	7.3	42
471	Dissolution-precipitation growth of uniform and clean two dimensional transition metal dichalcogenides. National Science Review, 2021, 8, nwaa115.	4.6	42
472	Self-Assembly and Cathodoluminescence of Microbelts from Cu-Doped Boron Nitride Nanotubes. ACS Nano, 2008, 2, 1523-1532.	7.3	41
473	Quenching of fluorescence of reduced graphene oxide by nitrogen-doping. Applied Physics Letters, 2012, 100, 233112.	1.5	41
474	Chiralityâ€Dependent Reactivity of Individual Singleâ€Walled Carbon Nanotubes. Small, 2013, 9, 1379-1386.	5.2	41
475	A nonstoichiometric SnO2â^'δ nanocrystal-based counter electrode for remarkably improving the performance of dye-sensitized solar cells. Chemical Communications, 2014, 50, 7020.	2.2	41
476	Effects of Carbon Nanotubes on Processing Stability of Polyoxymethylene in Meltâ^'Mixing Process. Journal of Physical Chemistry C, 2007, 111, 13945-13950.	1.5	40
477	One-Pot Synthesis of Metal–Carbon Nanotubes Network Hybrids as Highly Efficient Catalysts for Oxygen Evolution Reaction of Water Splitting. ACS Applied Materials & Interfaces, 2014, 6, 10089-10098.	4.0	40
478	<i>In Situ</i> Assembly of Multi-Sheeted Buckybooks from Single-Walled Carbon Nanotubes. ACS Nano, 2009, 3, 707-713.	7.3	39
479	2D hierarchical yolk-shell heterostructures as advanced host-interlayer integrated electrode for enhanced Li-S batteries. Journal of Energy Chemistry, 2019, 36, 64-73.	7.1	39
480	Synthesis of monolithic carbon aerogels with high mechanical strength via ambient pressure drying without solvent exchange. Journal of Materials Science and Technology, 2020, 50, 66-74.	5.6	39
481	Kinetic regulation of MXene with water-in-LiCl electrolyte for high-voltage micro-supercapacitors. National Science Review, 2022, 9, .	4.6	39
482	Identification of the constituents of double-walled carbon nanotubes using Raman spectra taken with different laser-excitation energies. Journal of Materials Research, 2003, 18, 1251-1258.	1.2	38
483	Poly(vinyl chloride) (PVC) Coated Idea Revisited: Influence of Carbonization Procedures on PVC-Coated Natural Graphite as Anode Materials for Lithium Ion Batteries. Journal of Physical Chemistry C, 2008, 112, 7767-7772.	1.5	38
484	A Comparative Study of the Structural, Electronic, and Vibrational Properties of NH ₃ BH ₃ and LiNH ₂ BH ₃ : Theory and Experiment. ChemPhysChem, 2009, 10, 1825-1833.	1.0	38
485	New Insight into the Interaction between Propylene Carbonate-Based Electrolytes and Graphite Anode Material for Lithium Ion Batteries. Journal of Physical Chemistry C, 2007, 111, 4740-4748.	1.5	37
486	Manganese-Catalyzed Surface Growth of Single-Walled Carbon Nanotubes with High Efficiency. Journal of Physical Chemistry C, 2008, 112, 19231-19235.	1.5	37

HUI-MING CHENG

#	Article	IF	CITATIONS
487	Catalytically enhanced dehydrogenation of Li–Mg–N–H hydrogen storage material by transition metal nitrides. Journal of Alloys and Compounds, 2009, 468, L21-L24.	2.8	37
488	Highly efficient H ₂ evolution over ZnO-ZnS-CdS heterostructures from an aqueous solution containing SO ₃ ²⁻ and S ²⁻ ions. Journal of Materials Research, 2010, 25, 39-44.	1.2	37
489	Direct Observation of Atomic Dynamics and Silicon Doping at a Topological Defect in Graphene. Angewandte Chemie - International Edition, 2014, 53, 8908-8912.	7.2	37
490	Double-Balanced Graphene Integrated Mixer with Outstanding Linearity. Nano Letters, 2015, 15, 6677-6682.	4.5	37
491	Direct writing of graphene patterns and devices on graphene oxide films by inkjet reduction. Nano Research, 2015, 8, 3954-3962.	5.8	37
492	An ultrasensitive molybdenum-based double-heterojunction phototransistor. Nature Communications, 2021, 12, 4094.	5.8	37
493	AÂ2D material–based transparent hydrogel with engineerable interference colours. Nature Communications, 2022, 13, 1212.	5.8	37
494	An environment-friendly microemulsion approach to α-FeOOH nanorods at room temperature. Materials Research Bulletin, 2006, 41, 2238-2243.	2.7	36
495	A simple and low-temperature hydrothermal route for the synthesis of tubular α-FeOOH. Materials Letters, 2007, 61, 4794-4796.	1.3	36
496	<i>In situ</i> electrical measurements of polytypic silver nanowires. Nanotechnology, 2008, 19, 085711.	1.3	36
497	Carbon nanotube-clamped metal atomic chain. Proceedings of the National Academy of Sciences of the United States of America, 2010, 107, 9055-9059.	3.3	36
498	Synthesis of Ultrahighâ€Quality Monolayer Molybdenum Disulfide through In Situ Defect Healing with Thiol Molecules. Small, 2020, 16, e2003357.	5.2	36
499	Preparation of carbon microcoils by catalytic decomposition of acetylene using nickel foam as both catalyst and substrate. Carbon, 2005, 43, 1874-1878.	5.4	35
500	Carbon nanotubes prepared by anodic aluminum oxide template method. Science Bulletin, 2012, 57, 187-204.	1.7	35
501	Enhanced photocatalytic hydrogen generation of mesoporous rutile TiO2 single crystal with wholly exposed {111} facets. Chinese Journal of Catalysis, 2015, 36, 2103-2108.	6.9	35
502	Flexible batteries ahead. National Science Review, 2017, 4, 20-23.	4.6	35
503	Water-assisted rapid growth of monolayer graphene films on SiO2/Si substrates. Carbon, 2019, 148, 241-248.	5.4	35
504	Properties and photodetector applications of two-dimensional black arsenic phosphorus and black phosphorus. Science China Information Sciences, 2021, 64, 1.	2.7	35

#	Article	IF	CITATIONS
505	Synthesis of rectangular cross-section AlN nanofibers by chemical vapor deposition. Chemical Physics Letters, 2005, 416, 171-175.	1.2	34
506	A simple solution route to controlled synthesis of ZnS submicrospheres, nanosheets and nanorods. Nanotechnology, 2006, 17, 4731-4735.	1.3	34
507	The effect of carbon particle morphology on the electrochemical properties of nanocarbon/polyaniline composites in supercapacitors. New Carbon Materials, 2011, 26, 180-186.	2.9	34
508	When two is better than one. Nature, 2013, 497, 448-449.	13.7	34
509	The rapid degradation of bisphenol A induced by the response of indigenous bacterial communities in sediment. Applied Microbiology and Biotechnology, 2017, 101, 3919-3928.	1.7	34
510	Highâ€Throughput Fabrication of Flexible and Transparent All arbon Nanotube Electronics. Advanced Science, 2018, 5, 1700965.	5.6	34
511	Allâ€Solidâ€State Planar Sodiumâ€ion Microcapacitors with Multidirectional Fast Ion Diffusion Pathways. Advanced Science, 2019, 6, 1902147.	5.6	34
512	Roles of multiwall carbon nanotubes in phytoremediation: cadmium uptake and oxidative burst in <i>Boehmeria nivea</i> (L.) Gaudich. Environmental Science: Nano, 2019, 6, 851-862.	2.2	34
513	The smart era of electrochemical energy storage devices. Energy Storage Materials, 2016, 3, 66-68.	9.5	33
514	Sensitive and selective detection of mercury ions based on papain and 2,6-pyridinedicarboxylic acid functionalized gold nanoparticles. RSC Advances, 2016, 6, 3259-3266.	1.7	33
515	A 3D Multifunctional Architecture for Lithium–Sulfur Batteries with High Areal Capacity. Small Methods, 2018, 2, 1800067.	4.6	33
516	A Rechargeable Quasi-symmetrical MoS2 Battery. Joule, 2018, 2, 1278-1286.	11.7	33
517	Extremely efficient flexible organic solar cells with a graphene transparent anode: Dependence on number of layers and doping of graphene. Carbon, 2021, 171, 350-358.	5.4	33
518	Anisotropic moiré optical transitions in twisted monolayer/bilayer phosphorene heterostructures. Nature Communications, 2021, 12, 3947.	5.8	33
519	An ultrathin and highly efficient interlayer for lithium–sulfur batteries with high sulfur loading and lean electrolyte. Journal of Materials Chemistry A, 2022, 10, 7653-7659.	5.2	33
520	Enhancing hydrogen peroxide activation of Cu Co layered double hydroxide by compositing with biochar: Performance and mechanism. Science of the Total Environment, 2022, 828, 154188.	3.9	33
521	Electrochemical Capacitors with Confined Redox Electrolytes and Porous Electrodes. Advanced Materials, 2022, 34, e2202380.	11.1	33
522	Title is missing!. Journal of Materials Science, 1999, 34, 827-834.	1.7	32

HUI-MING CHENG

#	Article	IF	CITATIONS
523	ZnS nanowires and their coaxial lateral nanowire heterostructures with BN. Applied Physics Letters, 2007, 90, 103117.	1.5	32
524	Achieving maximum photo-oxidation reactivity of Cs0.68Ti1.83O4â^'xNx photocatalysts through valence band fine-tuning. Catalysis Science and Technology, 2011, 1, 222.	2.1	32
525	All arbon Thinâ€Film Transistors as a Step Towards Flexible and Transparent Electronics. Advanced Electronic Materials, 2016, 2, 1600229.	2.6	32
526	Epitaxial growth of single-wall carbon nanotubes. Carbon, 2016, 102, 181-197.	5.4	32
527	Gradient Sn-Doped Heteroepitaxial Film of Faceted Rutile TiO ₂ as an Electron Selective Layer for Efficient Perovskite Solar Cells. ACS Applied Materials & Interfaces, 2019, 11, 19638-19646.	4.0	32
528	Chlorine capped SnO2 quantum-dots modified TiO2 electron selective layer to enhance the performance of planar perovskite solar cells. Science Bulletin, 2019, 64, 547-552.	4.3	32
529	Fast lithium ion transport in solid polymer electrolytes from polysulfide-bridged copolymers. Nano Energy, 2020, 75, 104976.	8.2	32
530	Semiconductor nanochannels in metallic carbon nanotubes by thermomechanical chirality alteration. Science, 2021, 374, 1616-1620.	6.0	32
531	Advantage of TiF3 over TiCl3 as a dopant precursor to improve the thermodynamic property of Na3AlH6. Scripta Materialia, 2007, 56, 361-364.	2.6	31
532	The facile synthesis of nickel silicide nanobelts and nanosheets and their application in electrochemical energy storage. Nanotechnology, 2008, 19, 165606.	1.3	31
533	Improving the photocatalytic activity of graphitic carbon nitride by thermal treatment in a high-pressure hydrogen atmosphere. Progress in Natural Science: Materials International, 2018, 28, 183-188.	1.8	31
534	Mitigating self-discharge of carbon-based electrochemical capacitors by modifying their electric-double layer to maximize energy efficiency. Journal of Energy Chemistry, 2019, 38, 214-218.	7.1	31
535	A flexible thermoelectric device based on a Bi2Te3-carbon nanotube hybrid. Journal of Materials Science and Technology, 2020, 58, 80-85.	5.6	31
536	Construction of sandwich-structured C/C-SiC and C/C-SiC-ZrC composites with good mechanical and anti-ablation properties. Journal of the European Ceramic Society, 2022, 42, 1219-1226.	2.8	31
537	Growth, metabolism of Phanerochaete chrysosporium and route of lignin degradation in response to cadmium stress in solid-state fermentation. Chemosphere, 2015, 138, 560-567.	4.2	30
538	Graphene based energy devices. Nanoscale, 2015, 7, 6881-2.	2.8	30
539	Molecular docking simulation on the interactions of laccase from Trametes versicolor with nonylphenol and octylphenol isomers. Bioprocess and Biosystems Engineering, 2018, 41, 331-343.	1.7	30
540	Control of Spatially Homogeneous Distribution of Heteroatoms to Produce Red TiO ₂ Photocatalyst for Visible‣ight Photocatalytic Water Splitting. Chemistry - A European Journal, 2019, 25, 1787-1794.	1.7	30

#	Article	IF	CITATIONS
541	Aligned Carbonâ€Based Electrodes for Fastâ€Charging Batteries: A Review. Small, 2021, 17, e2007676.	5.2	30
542	Highâ€Performance ITOâ€Free Perovskite Solar Cells Enabled by Singleâ€Walled Carbon Nanotube Films. Advanced Functional Materials, 2021, 31, 2104396.	7.8	30
543	Structure-related electrochemical behavior of sulfur-rich polymer cathode with solid-solid conversion in lithium-sulfur batteries. Energy Storage Materials, 2022, 45, 1144-1152.	9.5	30
544	Metallic Co and crystalline Co-Mo oxides supported on graphite felt for bifunctional electrocatalytic hydrogen evolution and urea oxidation. Journal of Colloid and Interface Science, 2022, 612, 413-423.	5.0	30
545	Identification of the conducting category of individual carbon nanotubes from Stokes and anti-Stokes Raman scattering. Physical Review B, 2000, 62, 5186-5190.	1.1	29
546	Double-walled carbon nanotubes synthesized using carbon black as the dot carbon source. Nanotechnology, 2006, 17, 3100-3104.	1.3	29
547	A film of rutile TiO2 pillars with well-developed facets on an $\hat{I}\pm$ -Ti substrate as a photoelectrode for improved water splitting. Nanoscale, 2012, 4, 3871.	2.8	29
548	A Double Support Layer for Facile Clean Transfer of Two-Dimensional Materials for High-Performance Electronic and Optoelectronic Devices. ACS Nano, 2019, 13, 5513-5522.	7.3	29
549	Decoupling of ion pairing and ion conduction in ultrahigh-concentration electrolytes enables wide-temperature solid-state batteries. Energy and Environmental Science, 2022, 15, 3379-3387.	15.6	29
550	Bandgap narrowing of titanium oxide nanosheets: homogeneous doping of molecular iodine for improved photoreactivity. Journal of Materials Chemistry, 2011, 21, 14672.	6.7	28
551	A graphene field-effect capacitor sensor in electrolyte. Applied Physics Letters, 2012, 101, .	1.5	28
552	A smart self-regenerative lithium ion supercapacitor with a real-time safety monitor. Energy Storage Materials, 2015, 1, 146-151.	9.5	28
553	Phase transition and in situ construction of lateral heterostructure of 2D superconducting $\hat{I}\pm/\hat{I}^2$ Mo ₂ C with sharp interface by electron beam irradiation. Nanoscale, 2017, 9, 7501-7507.	2.8	28
554	Transfer-free CVD graphene for highly sensitive glucose sensors. Journal of Materials Science and Technology, 2020, 37, 71-76.	5.6	28
555	High-efficiency and stable silicon heterojunction solar cells with lightly fluorinated single-wall carbon nanotube films. Nano Energy, 2020, 69, 104442.	8.2	28
556	Pushing the conductance and transparency limit of monolayer graphene electrodes for flexible organic light-emitting diodes. Proceedings of the National Academy of Sciences of the United States of America, 2020, 117, 25991-25998.	3.3	28
557	Giant magneto-birefringence effect and tuneable colouration of 2D crystal suspensions. Nature Communications, 2020, 11, 3725.	5.8	28
558	Simple approach to estimating the van der Waals interaction between carbon nanotubes. Physical Review B, 2006, 73, .	1.1	27

#	Article	IF	CITATIONS
559	A Raman probe for selective wrapping of single-walled carbon nanotubes by DNA. Nanotechnology, 2007, 18, 405706.	1.3	27
560	Enrichment of Semiconducting Single-Walled Carbon Nanotubes by Carbothermic Reaction for Use in All-Nanotube Field Effect Transistors. ACS Nano, 2012, 6, 9657-9661.	7.3	27
561	An integrated composite with a porous Cf/C-ZrB2-SiC core between two compact outer layers of Cf/C-ZrB2-SiC and Cf/C-SiC. Journal of the European Ceramic Society, 2015, 35, 1113-1117.	2.8	27
562	The effect of carbon support on the oxygen reduction activity and durability of single-atom iron catalysts. MRS Communications, 2018, 8, 1158-1166.	0.8	27
563	Recent Progress in 3D Printing of 2D Materialâ€Based Macrostructures. Advanced Materials Technologies, 2020, 5, 1901066.	3.0	27
564	Carbon Dotsâ€Decorated Carbonâ€Based Metalâ€Free Catalysts for Electrochemical Energy Storage. Small, 2021, 17, e2002998.	5.2	27
565	In Situ TEM Observations on the Sulfur-Assisted Catalytic Growth of Single-Wall Carbon Nanotubes. Journal of Physical Chemistry Letters, 2014, 5, 1427-1432.	2.1	26
566	Efficient organic photovoltaic cells on a single layer graphene transparent conductive electrode using MoO _x as an interfacial layer. Nanoscale, 2017, 9, 251-257.	2.8	26
567	Die wiederaufladbare Aluminiumbatterie: Möglichkeiten und Herausforderungen. Angewandte Chemie, 2019, 131, 12104-12124.	1.6	26
568	Development of Graphene-based Materials for Lithium-Sulfur Batteries. Wuli Huaxue Xuebao/ Acta Physico - Chimica Sinica, 2018, 34, 377-390.	2.2	26
569	2D Functional Minerals as Sustainable Materials for Magnetoâ€Optics. Advanced Materials, 2022, 34, e2110464.	11.1	26
570	Patterning of Waferâ€Scale MXene Films for Highâ€Performance Image Sensor Arrays. Advanced Materials, 2022, 34, e2201298.	11.1	26
571	Viscous Solvent-Assisted Planetary Ball Milling for the Scalable Production of Large Ultrathin Two-Dimensional Materials. ACS Nano, 2022, 16, 10179-10187.	7.3	26
572	Effects of Carbon Nanotubes and Metal Catalysts on Hydrogen Storage in Magnesium Nanocomposites. Journal of Nanoscience and Nanotechnology, 2006, 6, 494-498.	0.9	25
573	Enhanced Hydrogen Storage Properties of Liâ^'Mgâ^'Nâ^'H System Prepared by Reacting Mg(NH2)2 with Li3N. Journal of Physical Chemistry C, 2009, 113, 9944-9949.	1.5	25
574	Carbon-encapsulated NiO nanoparticle decorated single-walled carbon nanotube thin films for binderless flexible electrodes of supercapacitors. Journal of Materials Chemistry A, 2017, 5, 24813-24819.	5.2	25
575	High Yield Controlled Synthesis of Nano-Graphene Oxide by Water Electrolytic Oxidation of Glassy Carbon for Metal-Free Catalysis. ACS Nano, 2019, 13, 9482-9490.	7.3	25
576	Nickel phthalocyanine as an excellent hole-transport material in inverted planar perovskite solar cells. Chemical Communications, 2019, 55, 5343-5346.	2.2	25

#	Article	IF	CITATIONS
577	A Scalable Artificial Neuron Based on Ultrathin Two-Dimensional Titanium Oxide. ACS Nano, 2021, 15, 15123-15131.	7.3	25
578	Synthesis and Photoelectrochemical Behavior of Nitrogen-doped NaTaO3. Chemistry Letters, 2009, 38, 214-215.	0.7	24
579	3D graphene aerogel based photocatalysts: Synthesized, properties, and applications. Colloids and Surfaces A: Physicochemical and Engineering Aspects, 2020, 594, 124666.	2.3	24
580	Uniform polypyrrole electrodeposition triggered by phytic acid-guided interface engineering for high energy density flexible supercapacitor. Journal of Colloid and Interface Science, 2022, 611, 356-365.	5.0	24
581	Fabrication of carbon fibre-reinforced aluminium composites with hybridization of a small amount of particulates or whiskers of silicon carbide by pressure casting. Journal of Materials Science, 1992, 27, 3617-3623.	1.7	23
582	KH+Ti co-doped NaAlH4 for high-capacity hydrogen storage. Journal of Applied Physics, 2005, 98, 074905.	1.1	23
583	Direct formation of Na3AlH6 by mechanical milling NaHâ^Al with TiF3. Applied Physics Letters, 2005, 87, 071911.	1.5	23
584	Patterning flexible single-walled carbon nanotube thin films by an ozone gas exposure method. Carbon, 2013, 53, 4-10.	5.4	23
585	Open-pore LiFePO4/C microspheres with high volumetric energy density for lithium ion batteries. Particuology, 2015, 22, 24-29.	2.0	23
586	An integrated thermoelectric-assisted photoelectrochemical system to boost water splitting. Science Bulletin, 2020, 65, 1163-1169.	4.3	23
587	Catalystâ€Free Growth of Atomically Thin Bi ₂ O ₂ Se Nanoribbons for Highâ€Performance Electronics and Optoelectronics. Advanced Functional Materials, 2021, 31, 2101170.	7.8	23
588	Polarized Raman analysis of aligned double-walled carbon nanotubes. Physical Review B, 2005, 71, .	1.1	22
589	Improving Hydrogen Storage Performance of NaAlH4by Novel Two-Step Milling Method. Journal of Physical Chemistry C, 2007, 111, 4879-4884.	1.5	22
590	Thermal properties of nanocrystalline Al composites reinforced by AlN nanoparticles. Journal of Materials Research, 2009, 24, 24-31.	1.2	22
591	Maximizing the visible light photoelectrochemical activity of B/N-doped anatase TiO2 microspheres with exposed dominant {001} facets. Science China Materials, 2018, 61, 831-838.	3.5	22
592	Preparation of metallic single-wall carbon nanotubes. Carbon, 2019, 147, 187-198.	5.4	22
593	Carrier Trapping in Wrinkled 2D Monolayer MoS ₂ for Ultrathin Memory. ACS Nano, 2022, 16, 6309-6316.	7.3	22
594	Surface fractal dimension of single-walled carbon nanotubes. Physical Review B, 2004, 69, .	1.1	21

#	Article	IF	CITATIONS
595	Synthesis and field emission property of carbon nanotubes with sharp tips. New Carbon Materials, 2011, 26, 52-56.	2.9	21
596	Growth of metal-catalyst-free nitrogen-doped metallic single-wall carbon nanotubes. Nanoscale, 2014, 6, 12065-12070.	2.8	21
597	Batteries: A Graphene–Pureâ€Sulfur Sandwich Structure for Ultrafast, Longâ€Life Lithium–Sulfur Batteries (Adv. Mater. 4/2014). Advanced Materials, 2014, 26, 664-664.	11.1	21
598	Selective Growth of Metalâ€Free Metallic and Semiconducting Singleâ€Wall Carbon Nanotubes. Advanced Materials, 2017, 29, 1605719.	11.1	21
599	Manganese-enhanced degradation of lignocellulosic waste by Phanerochaete chrysosporium: evidence of enzyme activity and gene transcription. Applied Microbiology and Biotechnology, 2017, 101, 6541-6549.	1.7	21
600	Clean, fast and scalable transfer of ultrathin/patterned vertically-aligned carbon nanotube arrays. Carbon, 2018, 133, 275-282.	5.4	21
601	Improved Damping and High Strength of Graphene-Coated Nickel Hybrid Foams. ACS Applied Materials & Interfaces, 2019, 11, 42690-42696.	4.0	21
602	Layer-Stacking, Defects, and Robust Superconductivity on the Mo-Terminated Surface of Ultrathin Mo ₂ C Flakes Grown by CVD. Nano Letters, 2019, 19, 3327-3335.	4.5	21
603	Preparation of High Purity ZnO Nanobelts by Thermal Evaporation of ZnS. Journal of Nanoscience and Nanotechnology, 2006, 6, 704-707.	0.9	20
604	Dispersible percolating carbon nano-electrodes for improvement of polysulfide utilization in Li–S batteries. Carbon, 2015, 93, 161-168.	5.4	20
605	A Desolvated Solid–Solid Interface for a High apacitance Electric Double Layer. Advanced Energy Materials, 2019, 9, 1803715.	10.2	20
606	Confined van der Waals Epitaxial Growth of Two-Dimensional Large Single-Crystal In ₂ Se ₃ for Flexible Broadband Photodetectors. Research, 2019, 2019, 1-10.	2.8	20
607	Preparation and Fracture Behavior of Carbon Fiber/SiC Composites by Multiple Impregnation and Pyrolysis of Polycarbosilane. Journal of the Ceramic Society of Japan, 1998, 106, 1155-1161.	1.3	19
608	Zinc sulfide nanowire arrays on silicon wafers for field emitters. Nanotechnology, 2010, 21, 065701.	1.3	19
609	Design and construction of a film of mesoporous single-crystal rutile TiO2 rod arrays for photoelectrochemical water oxidation. Chinese Journal of Catalysis, 2015, 36, 2171-2177.	6.9	19
610	Spatial mobility fluctuation induced giant linear magnetoresistance in multilayered graphene foam. Physical Review B, 2016, 94, .	1.1	19
611	Integrated Paper-Based Flexible Li-Ion Batteries Made by a Rod Coating Method. ACS Applied Materials & Interfaces, 2019, 11, 46776-46782.	4.0	19
612	Tailoring microstructures of carbon fiber reinforced carbon aerogel-like matrix composites by carbonization to modulate their mechanical properties and thermal conductivities. Carbon, 2022, 196, 807-818.	5.4	19

#	Article	IF	CITATIONS
613	Electron microscopy study of Ti-doped sodium aluminum hydride prepared by mechanical milling NaHâ^•Al with Ti powder. Journal of Applied Physics, 2006, 100, 034914.	1.1	18
614	Selected absorption behavior of sulfur on single-walled carbon nanotubes by DFT. Chemical Physics Letters, 2008, 454, 305-309.	1.2	18
615	Long wavelength emissions of periodic yard-glass shaped boron nitride nanotubes. Applied Physics Letters, 2009, 94, 023105.	1.5	18
616	Growth of double-walled carbon nanotubes from silicon oxide nanoparticles. Carbon, 2013, 56, 167-172.	5.4	18
617	Correlation between topographic structures and local field emission characteristics of graphene-sheet films. Carbon, 2013, 61, 507-514.	5.4	18
618	Switching Photocatalytic H ₂ and O ₂ Generation Preferences of Rutile TiO ₂ Microspheres with Dominant Reactive Facets by Boron Doping. Journal of Physical Chemistry C, 2015, 119, 84-89.	1.5	18
619	A combined biological removal of Cd2+ from aqueous solutions using Phanerochaete chrysosporium and rice straw. Ecotoxicology and Environmental Safety, 2016, 130, 87-92.	2.9	18
620	Iron Oxide Nanoclusters Incorporated into Iron Phthalocyanine as Highly Active Electrocatalysts for the Oxygen Reduction Reaction. ChemCatChem, 2018, 10, 475-483.	1.8	18
621	UV-Epoxy-Enabled Simultaneous Intact Transfer and Highly Efficient Doping for Roll-to-Roll Production of High-Performance Graphene Films. ACS Applied Materials & Interfaces, 2018, 10, 40756-40763.	4.0	18
622	Grain Boundaries and Tilt-Angle-Dependent Transport Properties of a 2D Mo ₂ C Superconductor. Nano Letters, 2019, 19, 857-865.	4.5	18
623	The effect of Pt nanoparticles distribution on the removal of cyanide by TiO2 coated Al-MCM-41 in blue light exposure. Arabian Journal of Chemistry, 2019, 12, 957-965.	2.3	18
624	A flexible nickel phthalocyanine resistive random access memory with multi-level data storage capability. Journal of Materials Science and Technology, 2021, 86, 151-157.	5.6	18
625	Confined van der Waals Epitaxial Growth of Two-Dimensional Large Single-Crystal In ₂ Se ₃ for Flexible Broadband Photodetectors. Research, 2019, 2019, 2763704.	2.8	18
626	3D Printed Templateâ€Directed Assembly of Multiscale Graphene Structures. Advanced Functional Materials, 2022, 32, .	7.8	18
627	Stability of Supershort Single-Walled Carbon Nanotubes. Journal of Physical Chemistry B, 2005, 109, 12406-12409.	1.2	17
628	Controlled synthesis of quasi-one-dimensional boron nitride nanostructures. Journal of Materials Research, 2007, 22, 2809-2816.	1.2	17
629	Surface-restrained growth of vertically aligned carbon nanotube arrays with excellent thermal transport performance. Nanoscale, 2017, 9, 8213-8219.	2.8	17
630	Half-Metallicity in Co-Doped WSe ₂ Nanoribbons. ACS Applied Materials & Interfaces, 2017, 9, 38796-38801.	4.0	17

#	Article	IF	CITATIONS
631	Sandwich-structured C/C-SiC composites fabricated by electromagnetic-coupling chemical vapor infiltration. Scientific Reports, 2017, 7, 13120.	1.6	17
632	Degradation of di (2-ethylhexyl) phthalate in sediment by a surfactant-enhanced Fenton-like process. Chemosphere, 2018, 198, 327-333.	4.2	17
633	Lignocellulosic biomass derived N-doped and CoO-loaded carbocatalyst used as highly efficient peroxymonosulfate activator for ciprofloxacin degradation. Journal of Colloid and Interface Science, 2022, 610, 221-233.	5.0	17
634	Characteristics of several carbon fibrereinforced aluminium composites prepared by a hybridization method. Journal of Materials Science, 1994, 29, 4342-4350.	1.7	16
635	Heteroepitaxial Growth of Single-Walled Carbon Nanotubes from Boron Nitride. Scientific Reports, 2012, 2, 971.	1.6	16
636	Template synthesis of ultra-thin and short carbon nanotubes with two open ends. Journal of Materials Chemistry, 2012, 22, 15221.	6.7	16
637	Scalable residue-free graphene for surface-enhanced Raman scattering. Carbon, 2016, 98, 567-571.	5.4	16
638	In-situ imaging techniques for advanced battery development. Materials Today, 2022, 57, 279-294.	8.3	16
639	Boron nitride nanotubes filled with zirconium oxide nanorods. Journal of Materials Research, 2002, 17, 2761-2764.	1.2	15
640	MECHANICAL PROPERTIES OF SURFACTANT-COATING CARBON NANOFIBER/EPOXY COMPOSITE. International Journal of Nanoscience, 2002, 01, 425-430.	0.4	15
641	Raman evidence for atomic correlation between the two constituent tubes in double-walled carbon nanotubes. Physical Review B, 2006, 73, .	1.1	15
642	Synthesis, Purification and Opening of Short Cup-Stacked Carbon Nanotubes. Journal of Nanoscience and Nanotechnology, 2009, 9, 4554-4560.	0.9	15
643	Progress of graphene growth on copper by chemical vapor deposition: Growth behavior and controlled synthesis. Science Bulletin, 2012, 57, 2995-2999.	1.7	15
644	Realization of a non-markov chain in a single 2D mineral RRAM. Science Bulletin, 2021, 66, 1634-1640.	4.3	15
645	Iron-doped NiS2 microcrystals with exposed {0 0 1} facets for electrocatalytic water oxidation. Journal of Colloid and Interface Science, 2022, 608, 599-604.	5.0	15
646	Response of microorganisms to phosphate nanoparticles in Pb polluted sediment: Implications of Pb bioavailability, enzyme activities and bacterial community. Chemosphere, 2022, 286, 131643.	4.2	15
647	A potential link between the structure of iron catalysts and Fenton-like performance: from fundamental understanding to engineering design. Journal of Materials Chemistry A, 2022, 10, 12788-12804.	5.2	15
648	Preparation of carbon fibre reinforced aluminium via ultrasonic liquid infiltration technique. Materials Science and Technology, 1993, 9, 609-614.	0.8	14

#	Article	IF	CITATIONS
649	Preliminary investigation on the catalytic mechanism of TiF3 additive in MgH2–TiF3 H-storage system. Journal of Materials Research, 2007, 22, 1779-1786.	1.2	14
650	Improving the electrochemical properties of natural graphite spheres by coating with a pyrolytic carbon shell. New Carbon Materials, 2008, 23, 30-36.	2.9	14
651	Pyrolytic carbon-coated silicon/Carbon Nanotube composites: promising application for Li-ion batteries. International Journal of Nanomanufacturing, 2008, 2, 4.	0.3	14
652	Fermi level dependent optical transition energy in metallic single-walled carbon nanotubes. Carbon, 2011, 49, 4774-4780.	5.4	14
653	Diversity of ultrafast hot-carrier-induced dynamics and striking sub-femtosecond hot-carrier scattering times in graphene. Carbon, 2014, 72, 402-409.	5.4	14
654	Applications of carbon nanotubes and graphene produced by chemical vapor deposition. MRS Bulletin, 2017, 42, 825-833.	1.7	14
655	Six-membered-ring inorganic materials: definition and prospects. National Science Review, 2021, 8, nwaa248.	4.6	14
656	Lithium Metal Batteries: Ionâ€Dipole Chemistry Drives Rapid Evolution of Li Ions Solvation Sheath in Lowâ€Temperature Li Batteries (Adv. Energy Mater. 28/2021). Advanced Energy Materials, 2021, 11, 2170112.	10.2	14
657	Electrochemical Deposition of a Singleâ€Crystalline Nanorod Polycyclic Aromatic Hydrocarbon Film with Efficient Charge and Exciton Transport. Angewandte Chemie - International Edition, 2022, 61, .	7.2	14
658	An Interlayer Containing Dissociated LiNO ₃ with Fast Release Speed for Stable Lithium Metal Batteries with 400ÂWh kg ^{â~'1} Energy Density. Small, 2022, 18, .	5.2	14
659	SYNTHESIS OF WORMLIKE NANOPOROUS NICKEL OXIDE WITH NANOCRYSTALLINE FRAMEWORK FOR ELECTROCHEMICAL ENERGY STORAGE. International Journal of Nanoscience, 2004, 03, 321-329.	0.4	13
660	De-bundling of single-wall carbon nanotubes induced by an electric field during arc discharge synthesis. Carbon, 2014, 74, 370-373.	5.4	13
661	Bottom-Up Synthesis of 2D Transition Metal Carbides and Nitrides. , 2019, , 89-109.		13
662	Defective graphene as a high-efficiency Raman enhancement substrate. Journal of Materials Science and Technology, 2019, 35, 1996-2002.	5.6	13
663	Flexible organic photodetectors and their use in wearable systems. , 2022, 125, 103145.		13
664	Kinetics-Controlled Growth of Metallic Single-Wall Carbon Nanotubes from CoRe _{<i>x</i>} Nanoparticles. ACS Nano, 2022, 16, 232-240.	7.3	13
665	Enhanced H-storage property in Li–Co–N–H system by promoting ion migration. Journal of Alloys and Compounds, 2008, 466, L1-L4.	2.8	12
666	Probing quantum confinement of single-walled carbon nanotubes by resonant soft-x-ray emission spectroscopy. Applied Physics Letters, 2008, 93, .	1.5	12

#	Article	IF	CITATIONS
667	Effect of Li ₃ N additive on the hydrogen storage properties of Li-Mg-N-H system. Journal of Materials Research, 2009, 24, 1936-1942.	1.2	12
668	Structural evolution of carbon microcoils induced by a direct current. Carbon, 2009, 47, 670-674.	5.4	12
669	Amorphization and Directional Crystallization of Metals Confined in Carbon Nanotubes Investigated by in Situ Transmission Electron Microscopy. Nano Letters, 2015, 15, 4922-4927.	4.5	12
670	H2S + SO2 produces water-dispersed sulfur nanoparticles for lithium-sulfur batteries. Nano Energy, 2017, 41, 665-673.	8.2	12
671	Oriented outperforms disorder: Thickness-independent mass transport for lithium-sulfur batteries. Carbon, 2019, 154, 90-97.	5.4	12
672	Energy band edge alignment of anisotropic BiVO4 to drive photoelectrochemical hydrogen evolution. Materials Today Energy, 2019, 13, 205-213.	2.5	12
673	High-performance flexible resistive random access memory devices based on graphene oxidized with a perpendicular oxidation gradient. Nanoscale, 2021, 13, 2448-2455.	2.8	12
674	Collective Behavior Induced Highly Sensitive Magneto-Optic Effect in 2D Inorganic Liquid Crystals. Journal of the American Chemical Society, 2021, 143, 12886-12893.	6.6	12
675	Ultrastable Interfacial Contacts Enabling Unimpeded Charge Transfer and Ion Diffusion in Flexible Lithium″on Batteries. Advanced Science, 2022, 9, e2105419.	5.6	12
676	Effect of silicon additions on characteristics of carbon fiber reinforced aluminum composites during thermal exposure. Journal of Materials Research, 1996, 11, 1284-1292.	1.2	11
677	Light emission and degradation of single-walled carbon nanotube filament. Journal of Applied Physics, 2005, 98, 044306.	1.1	11
678	SYNTHESIS AND PROPERTIES OF ONE-DIMENSIONAL ALUMINUM NITRIDE NANOSTRUCTURES. Nano, 2007, 02, 307-331.	0.5	11
679	On Energy: Electrochemical capacitors: Capacitance, functionality, and beyond. Energy Storage Materials, 2017, 9, A1-A3.	9.5	11
680	Selective growth of semiconducting single-wall carbon nanotubes using SiC as a catalyst. Carbon, 2018, 135, 195-201.	5.4	11
681	Production of carbon dots during the liquid phase exfoliation of MoS2 quantum dots. Carbon, 2019, 155, 243-249.	5.4	11
682	High-throughput screening and machine learning for the efficient growth of high-quality single-wall carbon nanotubes. Nano Research, 2021, 14, 4610-4615.	5.8	11
683	Hybridization with SiC particulates to control the fibre volume fraction and improve the longitudinal tensile strength of carbon fibre-reinforced aluminium composites. Journal of Materials Science Letters, 1991, 10, 795-797.	0.5	10
684	Solid catalytic growth mechanism of micro-coiled carbon fibers. Science in China Series D: Earth Sciences, 2001, 44, 377-382.	0.9	10

HUI-MING CHENG

#	Article	IF	CITATIONS
685	How long can single-walled carbon nanotube ropes last under static or dynamic fatigue?. Applied Physics Letters, 2008, 92, 083105.	1.5	10
686	Synthesis of single-walled carbon nanotubes, their ropes and books. Comptes Rendus Physique, 2010, 11, 349-354.	0.3	10
687	Graphene Distributed Amplifiers: Generating Desirable Gain for Graphene Field-Effect Transistors. Scientific Reports, 2015, 5, 17649.	1.6	10
688	WB crystals with oxidized surface as counter electrode in dye-sensitized solar cells. Science Bulletin, 2017, 62, 114-118.	4.3	10
689	A carbon nanotube non-volatile memory device using a photoresist gate dielectric. Carbon, 2017, 124, 700-707.	5.4	10
690	A high tenacity electrode by assembly of a soft sorbent and a hard skeleton for lithium–sulfur batteries. Journal of Materials Chemistry A, 2017, 5, 22459-22464.	5.2	10
691	Ultrafast Transition of Nonuniform Graphene to High-Quality Uniform Monolayer Films on Liquid Cu. ACS Applied Materials & Interfaces, 2019, 11, 17629-17636.	4.0	10
692	Distinct superconducting properties and hydrostatic pressure effects in 2D $\hat{1}\pm$ - and $\hat{1}^2$ -Mo2C crystal sheets. NPG Asia Materials, 2020, 12, .	3.8	10
693	Stress release in high-capacity flexible lithium-ion batteries through nested wrinkle texturing of graphene. Journal of Energy Chemistry, 2021, 61, 243-249.	7.1	10
694	Dual-metal precursors for the universal growth of non-layered 2D transition metal chalcogenides with ordered cation vacancies. Science Bulletin, 2022, 67, 1649-1658.	4.3	10
695	Graphitization-induced microstructural changes in tetrahydrofuran-derived pyrolytic carbon spheres. Journal of Materials Research, 2006, 21, 2198-2203.	1.2	9
696	Magnetic nanocables—Silicon carbide sheathed with iron-oxide-doped amorphous silica. Applied Physics Letters, 2006, 88, 043105.	1.5	9
697	Contamination-free and damage-free patterning of single-walled carbon nanotube transparent conductive films on flexible substrates. Nanoscale, 2011, 3, 4571.	2.8	9
698	Wall-number selective growth of vertically aligned carbon nanotubes from FePt catalysts: a comparative study with Fe catalysts. Journal of Materials Chemistry, 2012, 22, 14149.	6.7	9
699	Oxygen Deficient Li ₄ Ti ₅ O ₁₂ for Highâ€rate Lithium Storage. Journal of the Chinese Chemical Society, 2012, 59, 1201-1205.	0.8	9
700	Lithium Storage Characteristics and Possible Applications of Graphene Materials. Acta Chimica Sinica, 2014, 72, 333.	0.5	9
701	Synthesis of high quality nitrogen-doped single-wall carbon nanotubes. Science China Materials, 2015, 58, 603-610.	3.5	9
702	Magnetotransport in Ultrathin 2-D Superconducting Mo2C Crystals. IEEE Transactions on Magnetics, 2017, 53, 1-4.	1.2	9

#	Article	IF	CITATIONS
703	Chirality transitions and transport properties of individual few-walled carbon nanotubes as revealed by in situ TEM probing. Ultramicroscopy, 2018, 194, 108-116.	0.8	9
704	The importance of H2 in the controlled growth of semiconducting single-wall carbon nanotubes. Journal of Materials Science and Technology, 2020, 54, 105-111.	5.6	9
705	Hierarchical urchin-like amorphous carbon with Co-adding anchored on nickel foam: A free-standing electrode for advanced asymmetrical supercapacitors and adsorbed Pb (II). Journal of Colloid and Interface Science, 2021, 603, 58-69.	5.0	9
706	FeCl3-functionalized graphene oxide/single-wall carbon nanotube/silicon heterojunction solar cells with an efficiency of 17.5%. Journal of Materials Chemistry A, 0, , .	5.2	9
707	Behaviour of carbon fibre reinforced Al–Si composites after thermal exposure. Materials Science and Technology, 1992, 8, 275-282.	0.8	8
708	Observations of novel carbon nanotubes with multiple hollow cores. Carbon, 2003, 41, 2477-2480.	5.4	8
709	Circular Graphene Platelets with Grain Size and Orientation Gradients Grown by Chemical Vapor Deposition. Advanced Materials, 2017, 29, 1605451.	11.1	8
710	Homogeneous boron doping in a TiO2 shell supported on a TiB2 core for enhanced photocatalytic water oxidation. Chinese Journal of Catalysis, 2018, 39, 431-437.	6.9	8
711	Singleâ€Atom Catalysts: Atomically Dispersed Transition Metals on Carbon Nanotubes with Ultrahigh Loading for Selective Electrochemical Carbon Dioxide Reduction (Adv. Mater. 13/2018). Advanced Materials, 2018, 30, 1870088.	11.1	8
712	Effects of domain structures on vortex state of two-dimensional superconducting Mo ₂ C crystals. 2D Materials, 2019, 6, 021005.	2.0	8
713	Lithium Batteries: The Regulating Role of Carbon Nanotubes and Graphene in Lithium–Ion and Lithium–Sulfur Batteries (Adv. Mater. 9/2019). Advanced Materials, 2019, 31, 1970066.	11.1	8
714	Controllable edge modification of multi-layer graphene for improved dispersion stability and high electrical conductivity. Applied Nanoscience (Switzerland), 2019, 9, 469-477.	1.6	8
715	Accurate structural descriptor enabled screening for nitrogen and oxygen vacancy codoped TiO2 with a large bandgap narrowing. Journal of Materials Science and Technology, 2022, 122, 84-90.	5.6	8
716	Some indications of the formation mechanism for double-walled carbon nanotubes by hydrogen-arc discharge. Carbon, 2005, 43, 2027-2030.	5.4	7
717	A self-similar array model of single-walled carbon nanotubes. Applied Physics Letters, 2005, 86, 203106.	1.5	7
718	PLATELET BORON NITRIDE NANOWIRES. Nano, 2006, 01, 65-71.	0.5	7
719	A comparison between field-emission properties of three one-dimensional carbon materials. Physica B: Condensed Matter, 2007, 396, 44-48.	1.3	7
720	ZnO microcolumns originated from self-assembled nanorods. Journal of Materials Science, 2008, 43, 1711-1715.	1.7	7

#	Article	IF	CITATIONS
721	Graphene Foams: Superhydrophobic Graphene Foams (Small 1/2013). Small, 2013, 9, 2-2.	5.2	7
722	Growth of tadpole-like carbon nanotubes from TiO2 nanoparticles. Carbon, 2013, 55, 253-259.	5.4	7
723	Metre-size single-crystal graphene becomes a reality. Science Bulletin, 2017, 62, 1039-1040.	4.3	7
724	High-Performance Sub-Micrometer Channel WSe ₂ Field-Effect Transistors Prepared Using a Flood–Dike Printing Method. ACS Nano, 2017, 11, 12536-12546.	7.3	7
725	Insights into the effect of chemical treatment on the physicochemical characteristics and adsorption behavior of pig manure-derived biochars. Environmental Science and Pollution Research, 2019, 26, 1962-1972.	2.7	7
726	Superhigh Uniform Magnetic Cr Substitution in a 2D Mo 2 C Superconductor for a Macroscopicâ€5cale Kondo Effect. Advanced Materials, 2020, 32, 2002825.	11.1	7
727	Largely Tunable Magneto-Coloration of Monolayer 2D Materials via Size Tailoring. ACS Nano, 2021, 15, 9445-9452.	7.3	7
728	Breaking the Rateâ€Integrity Dilemma in Largeâ€Area Bubbling Transfer of Graphene by Strain Engineering. Advanced Functional Materials, 2021, 31, 2104228.	7.8	7
729	Magnetic Doping Induced Superconductivity-to-Incommensurate Density Waves Transition in a 2D Ultrathin Cr-Doped Mo ₂ C Crystal. ACS Nano, 2021, 15, 14938-14946.	7.3	7
730	2D Functional Minerals as Sustainable Materials for Magnetoâ€Optics (Adv. Mater. 16/2022). Advanced Materials, 2022, 34, .	11.1	7
731	Engineering Graphene Grain Boundaries for Plasmonic Multi-Excitation and Hotspots. ACS Nano, 2022, 16, 9041-9048.	7.3	7
732	Preparation of isolated semiconducting single-wall carbon nanotubes by oxygen-assisted floating catalyst chemical vapor deposition. Chemical Engineering Journal, 2022, 450, 137861.	6.6	7
733	MICROSTRUCTURE AND RESISTIVITY OF CARBON NANOTUBE AND NANOFIBER/EPOXY MATRIX NANOCOMPOSITE. International Journal of Nanoscience, 2002, 01, 719-723.	0.4	6
734	Enhancement of Field Emission of CNTs Array by CO ₂ -Assisted Chemical Vapor Deposition. Journal of Nanoscience and Nanotechnology, 2009, 9, 3046-3051.	0.9	6
735	Ti-Zr-O Nanotube Arrays with Controlled Morphology, Crystal Structure and Optical Properties. Journal of Nanoscience and Nanotechnology, 2009, 9, 6501-6510.	0.9	6
736	Micro-Macroscopic Coupled Electrode Architecture for High-Energy-Density Lithium–Sulfur Batteries. ACS Applied Energy Materials, 2019, 2, 7393-7402.	2.5	6
737	Homologous gradient heterostructureâ€based artificial synapses for neuromorphic computation. InformaAnÃ-Materiály, 2023, 5, .	8.5	6
738	Evaluation of diameter distribution of inside cavities of open CNTs by analyses of nitrogen cryo-adsorption isotherm. Science Bulletin, 2001, 46, 1317-1320.	1.7	5

#	Article	IF	CITATIONS
739	Effect of geometrical parameters on the field-emission properties of single-walled carbon nanotube ropes. Journal of Materials Research, 2003, 18, 2188-2193.	1.2	5
740	Packing-dependent pore structures in single-walled carbon nanotube arrays. Applied Physics Letters, 2005, 87, 243109.	1.5	5
741	Ultrafast linear dichroism-like absorption dynamics in graphene grown by chemical vapor deposition. Journal of Applied Physics, 2014, 115, .	1.1	5
742	Transport Properties of Topological Semimetal Tungsten Carbide in the 2D Limit. Advanced Electronic Materials, 2019, 5, 1800839.	2.6	5
743	Reconstructed transparent conductive layers of fluorine doped tin oxide for greatly weakened hysteresis and improved efficiency of perovskite solar cells. Chemical Communications, 2020, 56, 129-132.	2.2	5
744	Fatigue Behaviour of Unidirectional Single-Walled Carbon Nanotube Reinforced Epoxy Composite under Tensile Load. Advanced Composites Letters, 2003, 12, 096369350301200.	1.3	4
745	Controlled growth of two-dimensional â€~single-crystal' hafnia networks by surface modulation. Nanotechnology, 2006, 17, 1207-1211.	1.3	4
746	Li–S Batteries: A Flexible Sulfurâ€Grapheneâ€Polypropylene Separator Integrated Electrode for Advanced Li–S Batteries (Adv. Mater. 4/2015). Advanced Materials, 2015, 27, 590-590.	11.1	4
747	Growth of nanocarbons by catalysis and their applications. MRS Bulletin, 2017, 42, 790-793.	1.7	4
748	Independent thickness and lateral size sorting of two-dimensional materials. Science China Materials, 2021, 64, 2739-2746.	3.5	4
749	Fractal effects on the measurement of the specific surface areas of single-walled carbon nanotubes. Carbon, 2005, 43, 1785-1787.	5.4	3
750	Controlling field-emission patterns of isolated single-walled carbon nanotube rope. Applied Physics Letters, 2005, 87, 043114.	1.5	3
751	Development of graphene-based materials for energy storage. , 2010, , .		3
752	Fabrication of a large-area, flexible and color-neutral single-wall carbon nanotube:sodium dodecylbenzene sulfonate/poly-(3,4-ethylenedioxythiophene):poly(4-styrenesulfonate) transparent conductive film having a new conduction mechanism. Carbon, 2014, 80, 112-119.	5.4	3
753	Electrochemical stability of graphene cathode for highâ€voltage lithium ion capacitors. Asia-Pacific Journal of Chemical Engineering, 2016, 11, 407-414.	0.8	3
754	Tunable In Situ Stress and Spontaneous Microwrinkling of Multiscale Heterostructures. Journal of Physical Chemistry C, 2019, 123, 26041-26046.	1.5	3
755	Electric Double Layer: A Desolvated Solid–Solid Interface for a High apacitance Electric Double Layer (Adv. Energy Mater. 12/2019). Advanced Energy Materials, 2019, 9, 1970037.	10.2	3
756	Mechanical-electro-magnetic coupling in strained bilayer CrI3. Science China Technological Sciences, 2020, 63, 1265-1271.	2.0	3

#	Article	IF	CITATIONS
757	Lithium Anodes: An Anionâ€Tuned Solid Electrolyte Interphase with Fast Ion Transfer Kinetics for Stable Lithium Anodes (Adv. Energy Mater. 14/2020). Advanced Energy Materials, 2020, 10, 2070063.	10.2	3
758	Superconductivity and High-Pressure Performance of 2D Mo ₂ C Crystals. Journal of Physical Chemistry Letters, 2021, 12, 2219-2225.	2.1	3
759	Electrochemical Deposition of a Singleâ€Crystalline Nanorod Polycyclic Aromatic Hydrocarbon Film with Efficient Charge and Exciton Transport. Angewandte Chemie, 2022, 134, .	1.6	3
760	Effect of C/SiC Volume Ratios on Mechanical and Oxidation Behaviors of Cf/C–SiC Composites Fabricated by Chemical Vapor Infiltration Technique. Acta Metallurgica Sinica (English Letters), 2022, 35, 801-811.	1.5	3
761	Fabrication of Largeâ€Area Uniform Nanometerâ€Thick Functional Layers and Their Stacks for Flexible Quantum Dot Lightâ€Emitting Diodes. Small Methods, 2022, 6, e2101030.	4.6	3
762	Honeycomb-like single-wall carbon nanotube networks. Journal of Materials Chemistry A, 2014, 2, 3308-3311.	5.2	2
763	Supercapacitors: Silicaâ€Mediated Formation of Nickel Sulfide Nanosheets on CNT Films for Versatile Energy Storage (Small 15/2019). Small, 2019, 15, 1970081.	5.2	2
764	Transport through a network of two-dimensional NbC superconducting crystals connected via weak links. Physical Review B, 2020, 101, .	1.1	2
765	Nanoribbons: Catalystâ€Free Growth of Atomically Thin Bi ₂ O ₂ Se Nanoribbons for Highâ€Performance Electronics and Optoelectronics (Adv. Funct. Mater. 31/2021). Advanced Functional Materials, 2021, 31, 2170230.	7.8	2
766	A photon-controlled diode with a new signal-processing behavior. National Science Review, 2022, 9, .	4.6	2
767	Microstructure of Silicon Nitride Ceramics and Morphology of Surface Damage Induced by Round Indenter. Journal of the Ceramic Society of Japan, 1994, 102, 350-354.	1.3	1
768	Oxidation of Carbon/B ₄ C/SiC/ZrB ₂ Composite in Moist Air at Elevated Temperature and the Thermodynamic Consideration. Journal of the Ceramic Society of Japan, 1994, 102, 925-929.	1.3	1
769	Carbon nanotubes enhanced hydrogen ab/desorption in Magnesium-based nanocomposites. , 2006, , .		1
770	Shaping different carbon nano- and submicro-structures by alcohol chemical vapor deposition. Journal of Materials Research, 2006, 21, 2504-2509.	1.2	1
771	Standard enthalpies of formation of finite-length (5, 5) single-walled carbon nanotube. Journal of Nanoparticle Research, 2008, 10, 1037-1043.	0.8	1
772	Raman Spectroscopy on Double-Walled Carbon Nanotubes. , 2008, , 29-39.		1
773	Photocatalysis: ZnO-CdS@Cd Heterostructure for Effective Photocatalytic Hydrogen Generation (Adv. Energy Mater. 1/2012). Advanced Energy Materials, 2012, 2, 2-2.	10.2	1
774	Defect and interlayer coupling tuned quasiparticle scattering in 2D disordered Mo2C superconducting microcrystals. Journal Physics D: Applied Physics, 2020, 53, 434002.	1.3	1

#	Article	IF	CITATIONS
775	Fabrication of high-conductivity RGO film at a temperature lower than 1500 źC by electrical current. Journal of Materials Science: Materials in Electronics, 2021, 32, 11727-11736.	1.1	1
776	Resonant Scattering in Proximity oupled Graphene/Superconducting Mo ₂ C Heterostructures. Advanced Science, 0, , 2201343.	5.6	1
777	Effect of SiO ₂ Type and Additives on the Reaction Products in SiO ₂ -Al-C-N ₂ System. Journal of the Ceramic Society of Japan, 1994, 102, 675-679.	1.3	Ο
778	MICROSTRUCTURE AND RESISTIVITY OF CARBON NANOTUBE AND NANOFIBER/EPOXY MATRIX NANOCOMPOSITE. , 2003, , .		0
779	SYNTHESIS AND CHARACTERIZATION OF CARBON NANOTUBES FOR HYDROGEN STORAGE. Series on Chemical Engineering, 2004, , 263-316.	0.2	Ο
780	Fabrication of Low-Voltage Electron Source from Patterned Arrays of Aligned Single-Walled Carbon Nanotube Ropes. Japanese Journal of Applied Physics, 2005, 44, 7713-7716.	0.8	0
781	Photocatalysis: Constructing a Metallic/Semiconducting TaB2/Ta2O5Core/Shell Heterostructure for Photocatalytic Hydrogen Evolution (Adv. Energy Mater. 12/2014). Advanced Energy Materials, 2014, 4, n/a-n/a.	10.2	Ο
782	Mobility controlled linear magnetoresistance with 3D anisotropy in a layered graphene pallet. Journal Physics D: Applied Physics, 2016, 49, 425005.	1.3	0
783	Arch-inspired super-elastic carbon materials. National Science Review, 2018, 5, 3-4.	4.6	Ο
784	Densification of MXene films by sequential bridging. National Science Review, 2022, 9, nwab195.	4.6	0
785	MECHANICAL PROPERTIES OF SURFACTANT-COATING CARBON NANOFIBER/EPOXY COMPOSITE. , 2003, , .		Ο
786	Controlled Shaping TiO2 for Efficient Photocatalysis. , 2012, , 43-72.		0
787	Nano-carbon Conductive Filmsâ \in "Fabrication, Processing and Devices. , 2013, , .		Ο
788	Synthesis and Properties of Quasi-One-Dimensional Nitride Nanostructures. , 2008, , 149-177.		0
789	Interface Design of Carbon Nano-Materials for Energy Storage. , 2008, , 41-47.		0
790	Effect of Mn And Zr on Hydrogen Absorption in Mg-Based Nanocomposites. NATO Science for Peace and Security Series C: Environmental Security, 2008, , 497-502.	0.1	0